HYPERSONIC WAVES IN CRYSTALS

V. V. LEMANOV and G. A. SMOLENSKIĬ

A. F. Ioffe Physico-technical Institute, USSR Academy of Sciences, Leningrad

Usp. Fiz. Nauk 108, 465–501 (November, 1972)

The fundamental results of recent research on the propagation of elastic microwaves (hypersonic waves) in crystals of various types are considered. The procedure for experiments with hypersonic waves is briefly described. The characteristics of the propagation of elastic waves in crystals (polarization, velocity, energy flux) and methods of their calculation are given. The principal mechanism of damping of hypersonic waves are considered, such as interactions with thermal phonons by the Akhiezer mechanism and by the Landau-Rumer mechanism, and interactions with free carriers and with defects. A separate chapter is devoted to problems of the propagation of hypersonic waves in magnetically-ordered crystals and their interactions with spin waves. The scattering of light by hypersonic waves is also considered, the singularities of this phenomenon are discussed, as is its use for the investigation of the characteristics of elastic-wave propagations. Some conclusions are drawn from the point of view of the prospects of using hypersonic methods in solid-state physics research.

CONTENTS

1. INTRODUCTION

MANY fundamental physical properties of crystals are connected with phonons. The interactions of phonons with phonons, electrons, magnons, and lattice defects underlie many important physical phenomena. The existing experimental methods for the investigation of processes in which phonons take part are mostly integral methods, which do not yield detailed information on the phonons. Such integral methods include, for example, measurements of the specific heat, the thermal conductivity, and thermal expansion. It is undoubtedly of interest to be able to investigate phonon processes by using "artificial" phonons of given frequency, wave vector, and polarization. Such a possibility can be realized with modern acoustic research methods, in which high-frequency elastic waves with frequencies exceeding 10^8 Hz (hypersonic waves) are used. The experimental use of such frequencies started relatively recently, following the publication of a paper by Baranskiĭ[1], who used the method of surface piezoelectric excitation to obtain elastic waves of frequency $\sim 10^9$ Hz in quartz crystals. The technique of hypersonic experiments has reached a high level by now and continues to develop. The frequency band up to 10^{10} Hz has been well mastered, and individual investigations of the propagation of elastic waves of still higher frequencies in crystals have been reported[2,3] Figure 1 shows an approximate form of the Debye spectrum of a crystal, in which hypersonic oscillations of a certain frequency are excited. The shaded region in the figure show the frequencies whose excitation is already possible at present. As can be seen from the figure, when compared of the most intense thermal phonons, which exist in a crystal without any action on our part, the artificial hypersonic phonons are so far of the low-frequency type, which the exception of the case of very low temperatures and the highest frequencies usable at the present time. There is no doubt, however, that further development of the experimental techniques will make it possible to obtain and investigate hypersonic waves with frequencies comparable with those of the most intense thermal phonons. It is of interest to note in this connection, recent experimental research on the propagation of high-frequency elastic waves excited in crystals by thermal pulses[4]. The method of thermal pulses makes it possible to obtain elastic waves with frequencies almost to 10^{12} Hz, but such experiments have been made so far only on a small number of crystals, and therefore are not considered in the present review.

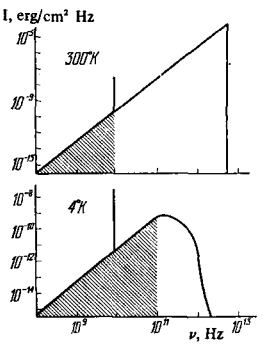

FIG. 1. Debye spectrum of a crystal in which hypersonic oscillations are excited at $\sim 10^{10}$ Hz.

Elastic waves with frequencies lower than 10^8 Hz have been in use for a long time to investigate physical properties of crystals, and it is therefore of interest to consider more specifically the advantages of research methods in which high-frequency (hypersonic) elastic waves are used.

The interactions of elastic waves with thermal phonons can be investigated only at sufficiently high elastic-wave frequencies. To investigate three-phonon interactions in which two thermal and one artificial phonon take part, it is necessary to satisfy the condition $\Omega\tau \gg 1$, where Ω is the frequency of the elastic waves and τ is the thermal-phonon relaxation time. The frequency Ω satisfying this condition depends, of course, on the temperature, but as a rule it exceeds 10^9 sec^{-1}. The investigation of the interaction of elastic waves with thermal phonons in the other limiting case $\Omega\tau \ll 1$ does not require high frequencies physically, but from the experimental point of view even this case can be investigated sufficiently well only at $\Omega \gtrsim 10^9$ sec^{-1}, since the contribution of the phonon-phonon interactions at lower frequencies small enough to be completely masked by other effects (diffraction losses, defects produced by working the crystals, etc.).

Methods that use elastic waves enable us to investigate the interactions of elastic waves with spin waves (magnons). Such processes become particularly important if the frequencies and the wave vectors of the elastic and spin waves are equal. When account is taken of the gap existing in the magnon spectrum, this condition also leads to the requirement $\Omega > 10^9$ sec^{-1}.

High-frequency elastic waves are frequently needed to study interactions with free carriers in semiconductors or with conduction electrons in metals[5], and to investigate acoustic and parametic resonance[6].

Very high frequencies are necessary also in the study of direct scattering of elastic waves by point defects in crystals, for only at very high frequencies it is possible to investigate the interaction of elastic waves with the soft phonon mode in phase transitions.

The use of hypersonic research methods is very interesting and fruitful in many regions of solid-state physics, and it is impossible to cover all these regions in a single review. We confine ourselves to a discussion of only several problems connected with the propagation of hypersonic waves in nonmetallic crystals. We consider in this review the main mechanisms of hypersonic-wave damping due to interactions with thermal phonons, with free carriers in piezosemiconductors, and with defects. In addition, we consider the interaction of hypersonic waves with spin waves in magnetically ordered crystals, and the scattering of light by hypersonic waves. We begin with a brief description of the procedures used in hypersonic experiments and present the basic information necessary to calculate the characteristics of the elastic-wave propagation in crystals.

2. EXPERIMENTAL PROCEDURE

Hypersonic waves are excited in crystals mainly with the aid of the piezoeffect. If the crystals in which the propagation of hypersonic waves is investigated have themselves a sufficiently strong piezoeffect, then the method of surface excitation of elastic waves directly in the crystals is used[1]. For crystals without the piezoeffect, plates or films of piezoconverters are attached to the investigated samples. The piezoconverter or crystal possessing the piezoeffect is placed in a coaxial line or in a microwave resonator, at the antinode of the electric field produced by an oscillator tuned to the corresponding frequency. In the case of surface excitation, the frequency of the elastic oscillations is determined only by the frequency of the generator, i.e., there are no resonance effects. When piezoelectric converters are used, the elastic oscillations are excited at resonant frequencies that are harmonics of the fundamental frequency of the converter. These frequencies are determined by the formula

$$\nu = (2n + 1)\,\nu_0 = (2n + 1)\,v/2d;$$

here v is the velocity of the elastic waves in the converter, ν_0 and d are the fundamental resonant frequency and the converter thickness, and n = 0, 1, 2, ...

Converters used in the form of plates are usually 50–100 μ thick. The average fundamental resonant frequency is 50–30 MHz in this case, so that to excite the hypersonic waves it is necessary to operate with very high harmonics. Film converters can have a thickness of approximately 1 μ, so that hypersonic oscillations can be excited at the fundamental resonant frequency of such converters.

Experiments with hypersonic waves are usually carried out in a pulsed regime (Fig. 2). A pulse of electromagnetic oscillations from a microwave generator is fed to the piezoelectric converter and is converted into a pulse of elastic oscillations of the same frequency. The elastic pulse propagates through the crystal and is partly reconverted into an electromagnetic pulse by a second converter or by the very first one operating "in reflection." The converted electromagnetic pulse is amplified in the receiver and registered with a pulse oscilloscope. The greater part of the elastic pulse is reflected in this case, and after passing again through the crystal it is registered anew, and this continues until the elastic pulses are attenuated by various damping mechanisms in the crystal. As a result, the oscilloscope displays a damped series of pulses, from which it is possible to determine both the damping of the elastic waves of the crystal and

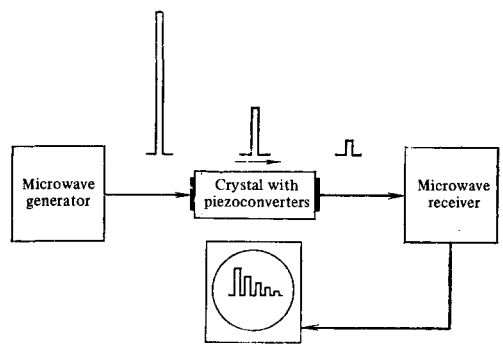

FIG. 2. Experimental setup.

their velocity. This, in general outline, is the procedure for experiments with hypersonic waves.

Let us examine now the main difficulties that arise in such experiments. One of the difficulties is the low efficiency of conversion of electromagnetic oscillations into elastic ones. The conversion losses frequently reach 30—40 dB, i.e., only 10^{-3}—10^{-4} of the electromagnetic-oscillation power is converted into elastic oscillations. Since the elastic waves are registered by reconverting them into electromagnetic oscillations, the total conversion loss is 60—80 dB. Such large losses are due to the difficulties of matching the microwave channel to the piezoconverter or the converter to the crystal, and also to the fact that when converters in the form of plates are used it becomes necessary to operate not at the fundamental resonant frequencies of these plates, but at high harmonics. Better results are obtained with film converters (cadmium or zinc sulfide, zinc oxide, etc.), which operate at the fundamental resonant frequency. With such converters, if the microwave channel is well matched to the converter, the conversion efficiency can be raised to several percent or even several dozen percent.

Other difficulties peculiar to hypersonic experiments are raised by the stringent requirements that the investigated samples must satisfy. At approximately 10^{10} Hz, the wavelength of the elastic oscillations is on the average 0.5 μ. The ends of the samples, i.e., the surfaces perpendicular to the direction of propagation of the elastic waves, must therefore be optically polished, otherwise these surfaces produce additional scattering of the elastic waves. The end surfaces must also be plane and parallel to a very high degree. Their deviation from parallelism reduces the observed number of elastic pulses and leads to a decrease and to a modulation of the pulse amplitudes, thereby greatly complicating the measurements. The pulses are attenuated and modulated because reflection takes place from non-parallel end faces alters the angle at which the plane elastic wave reaches the piezoconverter. As a result, the phase of the elastic wave is different, in different sections of the converter, thus causing a decrease of the signal in comparison with the case when the front of the elastic wave is parallel to the plane of the converter.

Estimates show that in many exact measurements of elastic-wave damping the deviation from parallelism must not exceed 2″. Samples for hypersonic measurements should thus be finished with "laser" accuracy. Of very great importance is also the quality of the junction between the converter and the sample. This junction is either by optical contact or with the aid of various adhesives (ceresin, vacuum lubricant, GKZh oil). The layer of the adhesive should be thin and homogeneous enough not to introduce additional losses. The problem of obtaining good acoustic contact is frequently simplified by using film converters that are deposited directly on the sample.

3. PROPAGATION OF ELASTIC WAVES IN CRYSTALS

In this chapter we present concise information on the calculation of such characteristics of elastic-wave propagation in crystals as the polarization, i.e., the direction of the displacement of the particles in the elastic waves, the velocity, and the direction of the energy flow in the elastic wave. Knowledge of these characteristics is essential for a correct organization of hypersonic experiments.

a) Velocities and polarizations of elastic waves. The question of calculating the velocity and polarization of an elastic wave in a crystal is considered in sufficient detail in a number of papers[7a,8,9]. We confine ourselves therefore to citing the fundamental equations necessary for such calculations.

Starting from the equation of motion for the elastic displacements

$$\rho\ddot{u}_i = c_{ihlm}\frac{\partial^2 u_l}{\partial x_k\,\partial x_m}$$

we can easily obtain the following equations for the calculation of the velocity and polarization of the elastic waves:

$$|\Gamma_{il} - X\delta_{il}| = 0 \tag{3.1}$$

and

$$\left.\begin{aligned} \gamma_y/\gamma_x &= [\Gamma_{xy}\Gamma_{xz} - \Gamma_{yz}(\Gamma_{xx} - X)]/[\Gamma_{yz}\Gamma_{xy} - \Gamma_{xz}(\Gamma_{yy} - X)], \\ \gamma_z/\gamma_x &= [\Gamma_{xy}\Gamma_{xz} - \Gamma_{yz}(\Gamma_{xx} - X)]/[\Gamma_{yz}\Gamma_{xz} - \Gamma_{xy}(\Gamma_{zz} - X)], \\ \gamma_x^2 + \gamma_y^2 + \gamma_z^2 &= 1; \end{aligned}\right\} \tag{3.2}$$

Here γ_i are the direction cosines of the displacement vector, $X = \rho V^2$ and $\Gamma_{il} = c_{iklm}\kappa_k\kappa_m$, where ρ is the density, v the velocity of the elastic waves, and κ_k the direction cosines of the wave vector.

An analysis of the solutions of the equations of motion shows[8,9] that for any propagation direction there exist in a crystal three independent elastic waves with displacements along mutually perpendicular directions. In the general case, none of the three displacement vectors coincides with the propagation direction.

A wave in which the displacement vector is closest to the propagation direction is customarily called quasilongitudinal, and the two other waves are called quasitransverse.

In any crystal there are, in addition, two types of special directions. Along one of them, which we shall call "pure," the elastic waves propagate in the form of pure modes, i.e., the displacement vector of one of the waves is parallel to the propagation direction (longitudinal wave) and the displacement vectors of the other two waves are perpendicular to this direction (transverse waves). The second special direction is characterized by the fact that one of the three waves propagating along this direction is purely transverse, and the other two are quasitransverse and quasilongitudinal. Some of the special directions in crystals can be obtained by starting from symmetry considerations. Thus, it is easily seen that the pure directions are the symmetry axes of any order, and also the directions perpendicular to the symmetry planes. We also note here that if the propagation direction coincides with a symmetry axis of order higher than second, such a direction is degenerate for the transverse waves, i.e., any displacement vector is possible for such waves in a plane perpendicular to the propagation direction, and the velocities of these waves are equal. Similarly, it follows from symmetry considerations that for any

propagation direction lying in the symmetry plane one of the waves must be purely transverse.

In addition to the pure directions determined on the basis of symmetry, other pure directions can also exist in a crystal.

To determine such directions, there is no need to solve the problem for each crystal separately. As is well known[10], the elastic properties of crystals are determined by nine symmetry groups. General formulas that determine the pure directions were obtained for these groups in[11a], where expressions are also given for the velocities and polarizations of the elastic waves along the pure directions.

b) **Energy flux.** The components of the energy flux vector in an elastic wave are[9] $P_i = -\dot{u}_k\sigma_{ik}$. Changing over from stresses to strains and assuming, as before, that the elastic wave is plane, we find that the direction cosines of the energy flux vector are proportional to

$$p_i \sim c_{iklm}\gamma_k\gamma_l\alpha_m. \tag{3.3}$$

In the general case, i.e., when an elastic wave propagates in an arbitrary direction, the direction of the energy flux does not coincide with the propagation direction, and the deviation can reach several dozen degrees. There are no such deviations in most cases of pure waves.

In experiments with hypersonic waves, the deviations of the energy flux from the propagation direction, which usually coincides with the sample axis, can cause errors in the measurements of the velocity and of the damping. It is therefore always preferable to use as the propagation directions in such experiments pure directions for which there are no deviations of the energy flux. This raises the question of how the characteristics of the elastic-wave propagation are affected by small and experimentally unavoidable inaccuracies in the sample orientation. This question is considered in[12]. It turns out that insignificant deviations of the sample axis from the pure direction can lead to appreciable deviations of the energy flux from the sample axis. Thus, an inaccuracy of 1° in a crystal of symmetry lower than cubic produces in individual cases an energy-flux deviation of 10% from the sample axis. These deviations are as a rule smaller in cubic crystals.

c) **Internal conical refraction and acoustic activity.** In concluding this section, we consider two interesting effects that accompany the propagation of transverse elastic waves in anisotropic media. The first effect is that in certain cases the energy flux in a purely transverse wave deviates from the propagation direction[9,12-14]. Such deviations occur, for example, when transverse waves propagate along a threefold axis in a crystal of any class. When the displacement vector in the transverse wave rotates around the threefold axis, the energy-flux vector describes a cone about this axis.

Using (3.3) we find, for example, that for propagation along the ⟨111⟩ direction in a cubic crystal, the expression for half the apex angle of the internal-refraction cone is

$$\alpha = \operatorname{arctg}\{(c_{11} - c_{12} - 2c_{44})/[\sqrt{2}\,(c_{11} - c_{12} + c_{44})]\}.$$

When the displacement vector in a transverse wave is in the {110} plane, the energy-flux vector lies in the same plane and makes an angle α with the propagation direction. When the displacement vector rotates around the propagation direction, the energy-flux vector also rotates, but in the opposite direction and at double the speed, describing in this case a cone about the threefold axis. A similar phenomenon takes place when an elastic wave propagates along a threefold axis in a crystal of lower symmetry. The internal conical refraction angle depends on the elastic constants of the crystal and can amount to ~10°. There have been a number of experimental studies of internal conical refraction[13,15], but this phenomenon has not yet been conclusively investigated.

Another interesting effect is a consequence of spatial dispersion of the elastic constants[16]. The influence of spatial dispersion can be quantitatively described by the coefficients of the linear terms in the expansions of the elastic constants in terms of the wavevector components. These coefficients form a fifth-rank tensor, and this leads to a number of complicated effects for elastic waves propagating in crystals of definite symmetry classes. When a transverse wave propagates along a threefold axis or an axis of higher order (in the absence of an inversion center and of symmetry planes), there should be observed effects analogous to optical activity produced by light propagating in the same directions. The normal elastic modes for such directions are left- and right-circularly polarized transverse waves with different propagation velocities, so that a linearly polarized transverse wave experiences rotation of the plane of polarization (natural acoustic activity. Acoustic activity should take place, for example, in the propagation along a threefold axis in crystals of quartz, tellurium (point group D_3), in bismuth germanate $Bi_{12}GeO_{20}$ (point group T), and others.

The acoustic activity is proportional to the square of the frequency[16] and is estimated at 1 rad/cm at 10^9 Hz. Calculation[16] shows that the specific acoustic activity of tellurium at this frequency is 165 deg/cm. The phenomenon of acoustic activity was first observed experimentally in[17] in the propagation of transverse waves along a threefold axis in a quartz crystal. The value obtained for the specific acoustic activity at 10^9 Hz, was approximately 100 deg/cm.

4. PRINCIPAL MECHANISMS OF DAMPING OF HYPERSONIC WAVES IN CRYSTALS

The propagation of hypersonic waves in crystals is accompanied by energy dissipation, i.e., the waves are damped when they propagate. In this chapter we consider the following principal hypersonic-wave damping mechanisms: interaction with thermal phonons, interaction with free carriers, and scattering by defects.

a) Interaction with thermal phonons. 1) The Akhiezer mechanism. The character of the interaction of the hypersonic waves with thermal phonons depends on the ratio of the frequency of the hypersonic waves Ω to the reciprocal thermal-phonon relaxation time $1/\tau$. If $\Omega \ll 1/\tau$, it is meaningless to consider individual interactions of hypersonic and thermal phonons, since

the energy of the hypersonic phonon turns out to be less than the uncertainty in the energy of the thermal phonon, $\hbar\Omega \ll \hbar/\tau$. The relation $\Omega\tau \ll 1$ can be rewritten in the $T \gg \tau$ or $\Lambda \gg l$, where T and Λ are the period and wavelength of the hypersonic oscillations, and l is the thermal-phonon mean free path. Under such conditions, the elastic wave will interact with an ensemble of thermal phonons as a whole, and the elastic deformations ϵ_{ik} in the hypersonic wave can be regarded as a classical field that leads to a change in the frequencies of the thermal phonons

$$\omega(\mathbf{q}, j) = \omega_0(\mathbf{q}, j)[1 - \gamma_{ik}(\mathbf{q}, j)\,\varepsilon_{ik}], \qquad (4.1)$$

where

$$\gamma^{ik}(\mathbf{q}, j) = -\frac{1}{\omega_0(\mathbf{q}, j)}\left[\frac{\partial\omega(\mathbf{q}, j)}{\partial\varepsilon_{ik}}\right]_{\varepsilon_{ik}=0}$$

is the Grüneisen coefficient and q and j are the wave vector and polarization of the phonons.

The change in frequency causes the distribution functions of the thermal phonons to deviate from their equilibrium values, the deviations being different for different phonon branches. The phonon-phonon collisions lead to relaxation of these deviations. During the relaxation, the entropy of the crystal increases and irreversible losses of the elastic-wave energy occur[18].

The problem of damping of elastic waves in crystals at $\Omega\tau \ll 1$ was first solved by Akhiezer[18] with the aid of the Boltzmann kinetic equation. The theory of damping by the Akhiezer mechanism was subsequently developed in[19,20].

Woodruff and Ehrenreich[20] present a detailed derivation of the expression for the damping of the elastic waves from a solution of the Boltzmann kinetic equation. This expression for the damping can be written in the form

$$A = \beta(\Omega^2 T/\rho v_0^3)\sum_{\mathbf{q}, j}\tau(\mathbf{q}, j)\gamma^2(\mathbf{q}, j)C(\mathbf{q}, j), \qquad (4.2)$$

where β is a numerical factor of the order of unity, Ω and v_0 are the frequency and velocity of the elastic waves, and C is the specific heat of the phonon branch (q, j). This formula does not make it possible, however, to calculate the magnitude and the temperature dependence of the damping of the elastic waves, since we have not enough knowledge of the characteristics τ, γ^2 and C of the phonon spectrum, so that approximate calculation methods must be employed at present. One such method, used in many papers to calculate damping in cubic crystals, was proposed by Mason[21a]. In this method it is assumed that the damping of the elastic waves is described by an effective relaxation time that is equal to or close in magnitude to the average relaxation time τ_{ph} of the thermal phonons; the latter is determined from the expression for the specific heat $\kappa = C\bar{v}^2\tau_{ph}/3$, where $\bar{v}$ is the average speed of sound in the Debye approximation and C is the specific heat of the crystal. This assumption concerning the relaxation time, which is common to all the approximate calculation methods, is of course difficult to justify[22], but one is nevertheless forced to use it.

The Grüneisen coefficients are calculated by using the elastic constants of second and third orders[11b]:

$$-\gamma_{ik}^r = \gamma_i\gamma_k + (\varkappa_m\varkappa_n/2c)(c_{ikmn} + c_{ikmpnq}\gamma_p\gamma_q), \qquad (4.3)$$

where γ and κ are the direction cosines of the particle displacement vector and of the wave vector, respectively, and $c = c_{mpnq}\kappa_m\kappa_n\gamma_p\gamma_q$. The index r denotes the phonon branch (q, j), the indices i and k pertain to the elastic wave, and the indices m, n, p, and q pertain to the considered phonon branch.

Assuming furthermore that the thermal energy is the same for all the phonon modes and is equal to $E_r = CTF/n$, where n is the number of modes considered and F is a slowly varying function of the temperature, equal to 0.25 at T = 0 and to 1 at $T \gg T_D$ (the Debye temperature), Mason obtained the following formula for the damping (for details see[21a]):

$$A = \beta(\Omega^2\tau_{ph}/\rho v_0^3)\,CTFn^{-1}\sum_{r=1}^{n}(\gamma_{ik}^r)^2. \qquad (4.4)$$

To calculate the damping in cubic crystals by means of this formula, Mason has proposed, by way of an approximation, to sum over 39 phonon modes (n = 39), corresponding to 13 pure directions in a cubic crystal: three ⟨100⟩, four ⟨111⟩, and six ⟨110⟩. The described method was used to calculate the damping in many crystals: Si, Ge[21a], LiF[23,21b], MgO[24b], and NaCl[25]. The experimental values of τ_{ph} (obtained from thermal conductivity) and elastic moduli of second and third orders were used. The calculated values of the damping agreed well with the experimental results. In particular, the calculation of the Grüneisen constants with the aid of the elastic constants explains the anisotropy of the damping in the crystals, i.e., the dependence of the damping on the elastic wave propagation direction, and also the difference between the damping of longitudinal and transverse elastic waves (see Fig. 3 and Table I, which lists the damping of elastic waves dB/μsec in certain cubic crystals; the elastic waves propagate along [110], the frequency is 100 MHz[1)], and the temperature is 300°K).

It follows from the table and from the figure that in many cases the damping depends strongly on the polarization of the elastic waves. In addition, as seen from Fig. 3, the frequency dependence of the damping is quadratic, as it should be in accordance with the Akhiezer damping mechanism. (The straight lines in Fig. 3 are drawn under the assumption that the damping has a quadratic frequency dependence.)

Mason's method was criticized in[22] because of a number of arbitrary assumptions made in the derivation of (4.4). The most serious objections concern the assumption that the thermal energy is equal for all phonon modes, which holds true only at sufficiently high temperatures, and the neglect of the possible dispersion of the Grüneisen constants, which are calculated in Mason's method from the elastic moduli and are considered to be independent of the temperature. These assumptions do not make it possible to use formula (4.4) to calculate the temperature dependence of the damping. More realistic is the approach of[26], where the contributions of the different phonon branches to (4.1) is taken into account with a weight

[1)] Damping values higher than ~10 dB/μsec were obtained by extrapolating the frequency dependences of the damping.

Table I

Crystal	T_D, °K	Polarization along [110]	[001]	[1$\bar{1}$0]	Crystal	T_D, °K	Polarization along [110]	[001]	[1$\bar{1}$0]
Ge	370	10	2	2	MgO	920	1.5	0.6	6.5
Si	650	6	1.6	1.6	BaF_2	280	3.5	2.4	2
					SrF_2	380	2.5	2.0	1.6
InSb	200	40	5	8	CaF_2	500	1.5	2.0	1.0
NaCl*)	310	15	2.5	25					
NaF	470	6.5	1.8	20	$Y_3Fe_5O_{12}$	500	1.0	0.3	0.3
LiF	700	2.5	1.0	12	$Y_3Al_5O_{12}$	700	0.4	0.3	0.3

*These values were obtained by extrapolating the data of [25].

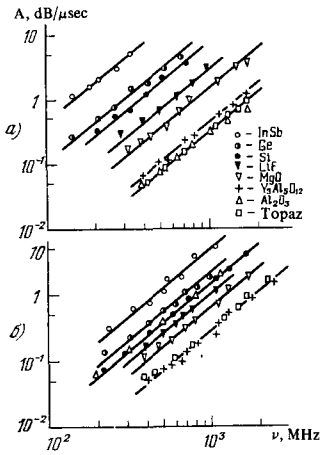

FIG. 3

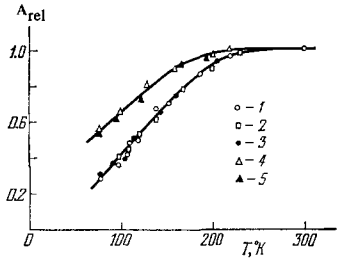

FIG. 4

FIG. 3. Frequency dependence of the damping of hypersonic waves propagating along a twofold symmetry axis at room temperature for longitudinal waves (a) and transverse waves with polarization along [001] (b).

FIG. 4. Temperature dependence of the damping of elastic waves of 1000 MHz frequency in silicon.

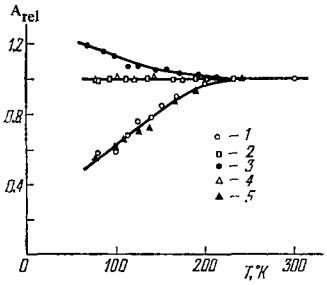

FIG. 5

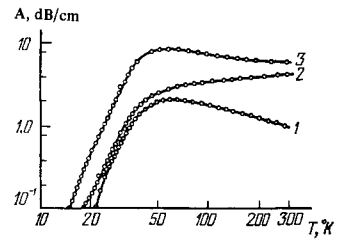

FIG. 6

FIG. 5. Temperature dependence of the damping of 1000-MHz elastic waves in LiF crystals.

FIG. 6. Temperature dependence of the damping of 1000-MHz elastic waves propagating along a twofold axis in quartz crystals for fast transverse (1), longitudinal (2), and slow transverse waves (3).

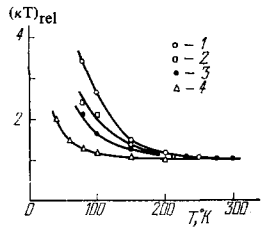

FIG. 7

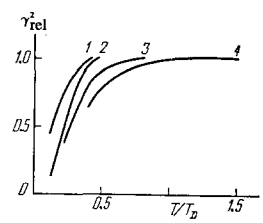

FIG. 8

FIG. 7. Temperature dependences of the product κT for crystals of topaz (1), Si (2), $Y_3Al_5O_{12}$ (3), and SiO_2 (4).

FIG. 8. Temperature dependences of the effective Grüneisen constant, calculated from formula (4.5) using the experimental data on the thermal conductivity and damping of hypersonic waves for LiF (1), Si (2), Ge (3), and InSb (4) longitudinal waves along [110]).

determined by the specific heat of the branch. The damping in a number of crystals (InAs, GeSi) was calculated by this method in[26]. This method, however, calls for definite information (or assumptions) about the specific heat of the phonon branches. In addition, the question of the possible dispersion of the Grüneisen constants (4.1) remains open as before. A seemingly more fruitful approach in this respect is one[27] in which the temperature dependences of the effective anharmonicity constants γ^2 are determined from the temperature dependences of the damping. Formula (4.2) is rewritten in the form

$$A = \beta\gamma^2 TC\tau_{ph}\Omega^2/\rho v_0^3,$$

where

$$\gamma^2 = C^{-1}\sum_{q,j}\gamma^2(q, j)\,C(q, j),$$

or, if we express τ_{ph} in terms of κ and neglect a numerical factor of order of unity,

$$A = \gamma^2\kappa T\Omega^2/\rho v_0^3\bar{v}^2. \qquad (4.5)$$

Comparing further (4.5) with the experimental data on the damping, we can determine the temperature dependence of the effective Grüneisen constant γ^2. According to (4.5), if γ^2 does not depend on the temperature, the damping and the product κT should have similar same temperature dependences, Figures 4–7 show such dependences for a number of crystals (in Figs. 4 and 5 the longitudinal waves propagate along [100] (1), [110] (2), and [111] (3), and the transverse waves propagate along [110] with polarization along [001] (4) and [110] (5); for Fig. 6[28], the Akhiezer criterion $\Omega\tau_{ph} < 1$ is satisfied at $T > 50°K$). The differences between the temperature dependences of the damping and the product κT can be related to a definite temperature dependence of γ^2 (Fig. 8). We note that the Akhiezer criterion $\Omega\tau_{ph} \ll 1$ is satisfied in a sufficiently wide range of frequencies and temperatures. In practically all crystals at room temperature and higher we have $\Omega\tau_{ph} < 1$ up to frequencies $\nu = \Omega/2\pi = 10^{10}$ Hz. Lowering the temperature causes a rather rapid growth of the relaxation time, but at the temperature of liquid nitrogen, for example, and at $\nu \lesssim 10^9$ Hz, this criterion is again satisfied for most crystals.

Many experimental data on the Akhiezer damping were analyzed in[29] from the viewpoint of the thermal properties of crystals. A distinct connection between the damping at 300°K and the thermal properties of the crystals was established. A connection of this type can be observed also for the crystals whose characteristics are listed in Table I.

Table I gives in addition to the elastic-wave damping also the Debye temperatures. A comparison of the Debye temperature with the damping shows that within each group of crystals having similar structures and properties there is a correlation between the damping and the Debye temperature, namely, the higher the Debye temperature the smaller the damping. This

result is indeed a consequence of the fact that the damping of the elastic wave is connected with the interaction with the thermal vibrations of the lattice. It is interesting to note that no such correlation exists for crystals having different structures and compositions. Thus, in the series of crystals Si, LiF, and $Y_3Al_5O_{12}$, which have approximately the same Debye temperature, the damping decreases by practically one order of magnitude on going from Si to $Y_3Al_5O_{12}$. This agrees with the conclusion proved in[29], that crystals of more complicated composition are characterized by smaller damping, other conditions being equal, owing to the decrease in the thermal-phonon relaxation time.

Summarizing, we can conclude that investigations of the damping by the Akhiezer mechanism make it possible in principle to determine such interesting characteristics of the phonon spectra as the anharmonicity constants and the relaxation times[27b], but the number of completed investigations in this direction is still quite small.

2) The Landau-Rumer mechanism. In those cases when the frequency of the hypersonic waves satisfies the inequality $\Omega\tau \ll 1$, the energy of the hypersonic phonons turns out to be larger than the uncertainty in the energy of the thermal phonons. The energy and momentum conservation laws then impose definite limitations on the possible interactions between the hypersonic and thermal phonons.

For three-phonon interactions, the conservation laws are

$$\Omega + \omega_1 = \omega_2, \quad \mathbf{q}_0 + \mathbf{q}_1 = \mathbf{q}_2, \tag{4.6}$$

where Ω and q_0 are the frequency and wave vector of the hypersonic phonon, and the subscripts 1 and 2 pertain to thermal phonons. Since the relation $\Omega\tau \gg 1$ is satisfied at low temperatures, Umklapp processes are not taken into account.

Recognizing that the momentum conservation law reduces to $q_0 + q_1 \geq q_2$, we can easily show that in an isotropic medium without dispersion only the following three-phonon interaction processes are possible: the process $L_0 + S_1 \rightarrow L_2$, in which a hypersonic phonon L_0 interacts with a transverse thermal phonon S_1 to produce a longitudinal thermal phonon L_1, is allowed for longitudinal hypersonic waves. For transverse hypersonic waves, the allowed processes are of the type

$$S_0 + L_1 \rightarrow L_2, \quad S_0 + S_1 \rightarrow L_2.$$

In addition to the indicated processes, collinear interaction processes, in which the wave vectors of all three interacting phonons are parallel, are also possible, namely

$$L_0 + L_1 \rightarrow L_2, \quad S_0 + S_1 \rightarrow S_2.$$

Recognizing further that the hypersonic phonons are of low frequency ($\Omega < kT/\hbar$) and they interact most effectively with high-frequency thermal phonons (ω_1, $\omega_2 \approx kT/\hbar$), we find that the thermal phonons participating in the interaction processes should have identical polarizations. This leaves for an isotropic elastic medium without dispersion only the following possible interactions:

for longitudinal waves

$$L_0 + L_1 \rightarrow L_2, \tag{4.7}$$

for transverse waves

$$S_0 + S_1 \rightarrow S_2, \quad S_0 + L_1 \rightarrow L_2. \tag{4.8}$$

It is easily seen that the relation $v_0 \leq v_{ph}$, where v_0 and v_{ph} are the velocities of the hypersonic and thermal phonons, is satisfied in processes (4.7) and (4.8). This relation, which follows from the conservation laws, can be illustratively explained to mean that the effective energy exchange between the hypersonic and thermal phonons occurs under conditions when the interacting phonons propagate "together" for a sufficiently long time. When $v_0 = v_{ph}$ this condition is satisfied only for thermal phonons propagating in the same direction as the hypersonic phonon (collinear interaction). When $v_0 < v_{ph}$ the thermal phonons that can interact with the hypersonic phonon propagate in a certain cone with angle $\alpha = \cos^{-1}(v_0/v_{ph})$.

If the dispersion of the phonon velocity is taken into account, then it turns out that collinear interactions are forbidden, since for any one phonon branch we always have $v_0 > v_{ph}$. The only process left from among the processes (4.7) and (4.8) is therefore

$$S_0 + L_1 \rightarrow L_2.$$

An expression for the damping of transverse elastic waves as a result of three-phonon processes was first derived by Landau and Rumer (see[30]). They used quantum-mechanical perturbation theory with allowance for the anharmonic third-order terms describing the three-phonon processes. The damping was found to be proportional to $A_S \sim \gamma^2 \Omega T^4$, where γ^2 is the anharmonicity constant. As for the longitudinal elastic waves, according to the theory their damping should be much smaller, since longitudinal waves cannot interact with high-frequency thermal phonons, and they interact only with phonons of comparable frequencies in processes of the $L_0 + S_1 \rightarrow L_2$ type. Experiments show, however, that the damping of longitudinal and transverse waves is close in magnitude, i.e., there exists for longitudinal waves a certain sufficiently effective mechanism of interaction with the thermal phonons. One can assume four-phonon processes to be possible interaction mechanisms, but calculations show[31a] that the contribution of these processes is very small. Another possible mechanism is the Herring mechanism[32], whereby anisotropy causes lines of intersection or tangency of different phonon branches in the wave-vector space to exist in crystals. This causes processes that are forbidden in an isotropic body to become allowed in an anisotropic crystal. Even this mechanism, however, results in a very small damping[33]. In addition, in both the four-phonon processes and in the Herring mechanism the resultant frequency and temperature dependences of the damping differ from those observed experimentally[33].

The effect of the finite relaxation time of the thermal phonon on the possible interaction processes was first taken into account in[34]. A finite relaxation time leads to an uncertainty in the energy of the thermal phonons, $\Delta E \sim \hbar/\tau$. If this uncertainty exceeds the energy "unbalance" in the conservation law for a given forbidden process, then this process becomes allowed.

According to (4.6), the energy "unbalance" in a process for which the conservation law is not satisfied is

$$\hbar\Delta\Omega = \hbar(\Omega + \omega_1 - \omega_2) = \hbar\Omega[1 - (\omega_2 - \omega_1)\Omega^{-1}].$$

Since

$$(\omega_2 - \omega_1)/\Omega = (v_{ph}/v_0)(q_2 - q_1)/q_0 \approx (v_{ph}/v_0)\cos\alpha,$$

where α is the angle between $\mathbf{q}_0$ and $\mathbf{q}_2$, it follows that

$$\hbar\Delta\Omega = \hbar\Omega[1 - (v_{ph}/v_0)\cos\alpha].$$

The smallest "unbalance" occurs at $\alpha = 0$ (collinear process):

$$\hbar\Delta\Omega_{min} = \hbar\Omega[1 - (v_{ph}/v_0)].$$

Recognizing further that $(v_{ph}/v_0) = (1 - bq^2a^2)$, where b is a numerical factor and a is the lattice parameter, and that $q^2a^2 \approx q^2/q^2_{max} \approx (T/T_D)^2$, we obtain ultimately

$$\hbar\Delta\Omega_{min} \approx \hbar\Omega(T/T_D)^2.$$

If $\hbar/\tau \gg \hbar\Omega(T/T_D)^2$, then the collinear processes (4.7) turn out to be possible.

Thus, if $\Omega\tau \ll (T_D/T)^2$ (but at the same time $\Omega\tau \gg 1$), then the conservation laws impose no limitations on the collinear interaction of hypersonic waves with high-frequency thermal phonons. The damping is calculated in this case also by quantum-mechanical perturbation theory[30], but one introduces into the expression for the transition probability not the δ-function $\delta(E_i - E_f)$, which gives the energy conservation law, but the smoother function $(\hbar/\pi)\tau/[\hbar^2 + (E_i - E_f)^2\tau^2]$. The damping of the longitudinal waves turn out to be proportional[35] to $A_L \sim \gamma^2\Omega T^4$, just as for the transverse ones.

We note that the condition $\Omega\tau \gg 1$ is usually satisfied at $T \lesssim 0.1T_D$, i.e., the inequality $\Omega\tau \ll (T_D/T)^2$ is always possible in a definite range of frequencies and temperatures. When the temperature is lowered, the thermal-phonon relaxation time, which is determined mainly by the normal processes, increases more rapidly than T^{-2},[36], and the inequality $\Omega\tau < (T_D/T)^2$ no longer holds. In the opposite limiting case, $\Omega\tau \gg (T_D/T)^2$, the uncertainty in the energy of the thermal phonons becomes less than the "unbalance" of the energy in the process (4.7), the process becomes forbidden, and the damping decreases abruptly. Calculation[37] shows that the damping of longitudinal waves does not depend in this case on the frequency and is proportional to $A_L \sim T^2/\tau$. Inasmuch as the steepest temperature dependence of τ corresponds to[36] T^{-5}, we have $A_L \sim T^7$ (see also[31a]. In analogy to the longitudinal waves, the finite relaxation time also lifts the forbiddenness of the collinear interaction $S_0 + S_1 \rightarrow S_2$ for the transverse waves.

In[35,37] they considered also the influence of the finite relaxation time on the process $L_0 + S_1 \rightarrow S_2$. This process does not satisfy the conservation laws at all, whether or not dispersion in present in the medium. Nevertheless, it is shown in[37] that when the finite τ is taken into account this process can make a noticeable contribution to the damping. In this case the damping turns out to be likewise independent of the frequency and proportional to T^4/τ, which can lead to as steep a temperature dependence of the damping as T^9.

We present now formulas for hypersonic-wave damping due to the considered three-phonon processes, in the same form as given in[35,37]. The formulas were obtained by perturbation theory with allowance for the finite relaxation time of the thermal phonons:

transverse waves, processes $S_0 + L_1 \rightarrow L_2$ and $S_0 + S_1 \rightarrow S_2$:

$$A_S = (\pi^2\hbar\Omega/60\rho^3)(kT/\hbar)^4\{(F_1^2/\bar{v}^{10}) + F_2^2/v_S^{10})[(\pi/2) - \operatorname{arctg} 0{,}32\Omega\tau X]\}, \quad (4.9)$$

Longitudinal waves, processes $L_0 + S_1 \rightarrow S_2$ and $L_0 + L_1 \rightarrow L_2$:

$$A_L = (\pi^2\hbar/30\rho^3)(kT/\hbar)^4\{\tau^{-1}[F_3^2/v_L v_S^5(v_L^2 - v_S^2)] + (\Omega F_4^2/2v_L^{10})[(\pi/2) - \operatorname{arctg} 0{,}32\Omega\tau X]\}; \quad (4.10)$$

here F is the anharmonicity constant (the phonon-phonon interaction constant) and is a combination of the second- and third-order elastic moduli:

$$F = \gamma_{0i}\gamma_{1j}\gamma_{2k}\varkappa_{0l}\varkappa_{1m}\varkappa_{2n}(c_{iljmkn} + c_{ilmn}\delta_{jk} + c_{jmln}\delta_{ik} + c_{knlm}\delta_{ij}),$$

where γ and $\varkappa$ are the direction cosines of the particle displacement vector and the wave vector, while the indices 0, 1, and 2 pertain, as before, to the hypersonic and thermal phonons, respectively. The parameter X is given by $X = k^2T^2a^2/\hbar^2v^2$, and its order of magnitude is $X \approx (T/T_D)^2$.

From formulas (4.9) and (4.10), in accordance with the already considered results, it follows that when $\Omega\tau \ll (T_D/T)^2$ (relatively high temperature and low-frequencies) the damping of the hypersonic waves is proportional to ΩT^4. At $\Omega\tau \gg (T_D/T)^2$ (lower temperatures and high frequencies), the damping of the longitudinal waves is independent of the frequency and depends on the temperature like T^n, where n ranges from 7 to 9, depending on the relative contributions of the first and second terms in (4.10). As to the transverse waves, their damping is proportional in this case to $\Omega^m T^n$, where m ranges from 1 to 0 and n from 4 to 7, depending on the relative contributions of the terms in (4.9).

We now compare the conclusions of the theory with the experimental results. Damping of hypersonic waves in crystals at $\Omega\tau \ll 1$ was investigated in a number of papers. In[23,33,38,39] they investigated the cubic crystals LiF, CaF_2, MgO, and others. The lower-symmetry crystals SiO_2, Al_2O_3, and TiO_3 were investigated in[24c,28,33,35,37,38,40-42] The hypersonic-wave damping was measured at frequencies from 5×10^8 to 10^{10} Hz and at temperatures from 100 to 4.2°K. The most general frequency and temperature dependences found for the damping in the cited papers consist in the following: the damping of transverse waves is proportional to ΩT^4 in a wide range of temperatures and frequencies. For longitudinal waves at relatively high temperatures, the damping is also proportional to ΩT^4, and when the temperature is lowered the damping ceases to depend on the frequency and becomes proportional to T^7. At still lower temperatures in certain crystals, the damping of the longitudinal waves turns out to be proportional to T^9. Such a sharp temperature dependence of the damping was observed in the crystals LiF[39], SiO_2[24c,40], Al_2O_3[37,41], TiO_2[42]. By way of illustration, Fig. 9 shows the temperature dependence of the damping of longitudinal and transverse waves in Al_2O_3[41]. Figure 6 shows the temperature

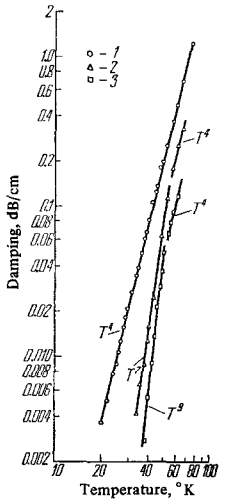

FIG. 9. Temperature dependence of the damping of elastic 1000-MHz waves propagating in Al_2O_3 along the twofold axis: 1) slow transverse, 2) fast transverse, 3) longitudinal.

dependence of the damping in quartz crystals[28] (the condition $\Omega\tau > 1$ is satisfied in this case at temperatures below 40°K).

Thus, the character of the frequency and temperature dependences of the damping agrees well in general with the predictions of theory. The absolute value of the damping, calculated from formulas (4.9) and (4.10), also agrees satisfactorily with experiment. The latter, however, should not be assigned too much significance, since the formulas for the damping contain such parameters as the anharmonicity constant F, the average elastic-wave velocity v, and the relaxation time τ, the values of which are not known accurately. Consequently, the only criterion for the correctness of the considered theory is for the time being the agreement between the theoretical and experimental temperature dependence of the damping.

It must also be borne in mind in the analysis of the experimental results that the temperature dependence of the damping can be strongly influenced both by singularities of the phonon spectrum[47] and by the anisotropy of the phonon-phonon interaction constants[44].

We have considered so far the case $\hbar\Omega \ll kT$. In[2] they investigated the damping of longitudinal waves in quartz crystals at a frequency 7×10^{10} Hz corresponding to $\hbar\Omega \approx kT$ at helium temperatures, when both three-phonon decay processes of the type $L_0 \rightarrow S_1 + L_2$ and processes of the type $L_0 + S_1 \rightarrow L_2$ are effective. In the experiment of[2], the observed damping depended on the temperature like T^4 as against T^7 or T^9 at lower temperatures. Such a dependence is possibly due just to the additional interaction processes that increase the damping at low temperatures. The case $\Omega\hbar \approx kT$ was not investigated in greater detail.

b) **Interaction with free carriers.** A contribution to the damping of hypersonic waves in crystals can be made not only by scattering by thermal phonons, but also by interaction with free carriers. For piezoelectric crystals, such an interaction is due to the fact that the propagation of elastic wave in the piezoelectric is accompanied by alternating electric fields that act on the free carriers. In addition to this interaction mechanism, which operates only in piezoelectrics, coupling between the elastic waves and the carriers may be produced by a deformation potential, i.e., to a change in the width of the band by elastic deformation. The latter mechanism, however, usually leads to a damping that is much smaller than the damping due to scattering by thermal phonons. As to piezoelectric semiconductors, their main damping mechanism is frequently the electron-phonon interaction.

The theory of electron-phonon interaction in piezosemiconductors was developed by Gurevich, Hutson, and White[45a,46].

The main results of the theory are obtained by solving the following system of equations[46]

$$T = c\frac{\partial u}{\partial x} - \beta E, \quad D = \beta\frac{\partial u}{\partial x} + \varepsilon E, \quad \rho\ddot{u} = \frac{\partial T}{\partial x},$$

$$\frac{\partial D}{\partial x} = -en, \quad \frac{\partial J}{\partial x} = e\frac{\partial n}{\partial t}, \quad J = e(n_0 + n)\mu E + e\mathcal{D}\frac{\partial n}{\partial x}.$$

These equations, written down for the one-dimensional case, are respectively the equation of state for the piezoelectric, the equation of motion of elasticity theory, the Poisson equation, the continuity equation, and the equation for the current. Here e is the electron charge, β and ϵ are the piezoelectric and dielectric constants, μ and D are the mobility and the diffusion coefficient of the carriers, n_0 is their equilibrium concentration, and n is the deviation from the equilibrium concentration, and is caused by the elastic wave. In the linear approximation, this system of equations reduces to the equation of motion

$$\rho\ddot{u} = c_{\text{eff}}\frac{\partial^2 u}{\partial x^2},$$

where c_{eff} is the complex elastic modulus, whose imaginary part determines the damping of the elastic waves due to the coupling with the carrier[46]:

$$A\ (\text{dB}/\mu\,\text{sec}) = 4.34\cdot 10^{-6}\chi^2\,[\Omega^2\tau_c/(1+\Omega^4\tau_D^2\tau_c^2+2\Omega^2\tau_D\tau_c+\Omega^2\tau_c^2); \quad (4.11)$$

here $\chi = (\beta^2/c\epsilon)^{1/2}$ is the electromechanical coupling constant, $\tau_C = \epsilon/\sigma$ is the Maxwellian relaxation time, and $\tau_D = kT/ev^2$ is the "diffusion time," where σ is the electron conductivity and v is the velocity of the elastic waves.

Thus, the damping of the elastic waves is in general a complicated function of the electric characteristics of the semiconductor. At certain ratios of the frequency Ω to the elastic waves and the characteristic parameters τ_C and τ_D, formula (4.11) assumes a simpler form. We consider in this connection two limiting cases. If all the terms in the denominator of (4.11) are small in comparison with unity ($\Omega\tau < 1$), then the damping turns out to be

$$A = 4.34\cdot 10^{-6}\,\chi^2\varepsilon\Omega^2\rho, \quad (4.12)$$

where ρ is the electric resistivity. The damping is proportional in this case to the square of the elastic-wave frequency to the resistivity of the crystal, In the other limiting case, when $\Omega\tau_C > 1$ and $\Omega\tau_D < 1$, we have

$$A = 4.34\cdot 10^{-6}\chi^2\sigma/\varepsilon, \quad (4.13)$$

i.e., the damping does not depend on the frequency and is proportional to the electric conductivity.

Elastic-wave damping due to interaction with free carriers was investigated in a number of crystals such as CdS[47], GaAs[48], and Te[49]. The experimental results are described well by formula (4.11). By way of

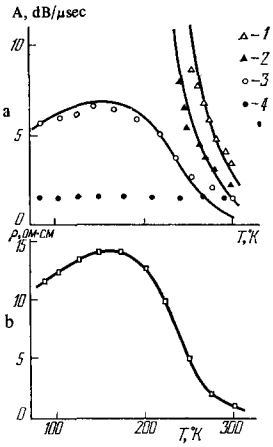

FIG. 10

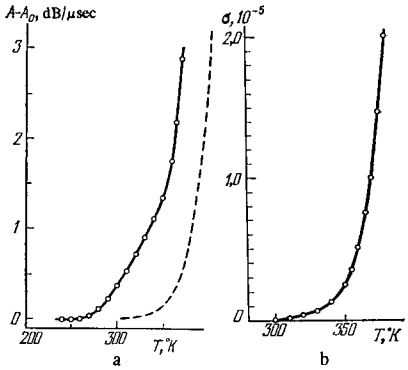

FIG. 11

FIG. 10. Temperature dependences of the damping of longitudinal elastic waves (a) and of the electric resistivity (b) in tellurium crystals.

FIG. 11. Temperature dependence of the damping of longitudinal 100-MHz waves (a) and of the electric conductivity (b) of lithium niobate crystals reduced in a hydrogen atmosphere (σ is in units of $\Omega^{-1}\,cm^{-1}$).

example we present the temperature dependences of the damping of longitudinal waves in tellurium crystals[49] (Fig. 10a) and in lithium niobate crystals[50] (Fig. 11a).

In the case of tellurium (point group D_3) the piezoelectrically active elastic waves, i.e., the waves that produce electric fields in the crystal, are longitudinal waves along the x (C_2) axis. Consequently, the free carriers can contribute to the damping of these waves. At $\sim 10^8$ Hz, this contribution, as shown by measurements of the electric properties, should be described by formula (4.12). The experimental points in Fig. 10a actually coincide with the theoretical relation (12), which is represented by the solid curves (for an undoped sample; 1, 2, and 3 correspond to 200, 150, and 90 MHz, respectively).

The points 4 for 90 MHz in this figure pertain to a doped sample with carrier density 3.5×10^{-16} cm^{-3} at 77°K. The small value of the damping and its independence of the temperature are connected in this case with the fact that the decrease of the resistivity, due to doping, decreases the contribution of the carriers (4.12) to a value small in comparison with the lattice damping. The damping of the longitudinal waves along the z (C_3) axis also turns out to be independent of the temperature (in both pure and in doped samples), since these waves are not piezoelectrically active, i.e., they do not interact with the carriers[49].

Figure 11 pertains to lithium niobate crystals reduced in a hydrogen atmosphere. According to[51], the electric conductivity of such crystals is of the n-type. Measurements of the electric properties show that the characteristic parameters τ_C and τ_D of the reduced crystals are such that the damping connected with the free carriers should be determined by formula (4.13) in the frequency and temperature interval investigated in[50]. In the case of lithium-niobate crystals (point group C_{3v}), the piezoelectrically active waves are longitudinal waves along the z (C_3) axis. It is the temperature dependence of the damping of these waves which is shown in Fig. 11a. It follows from it that when the electric conductivity of the crystals increases with increasing temperature, the damping also increases. When the degree of reduction decreases, as shown by the measurements, the electric conductivity decreases and the growth of the damping begins at higher temperatures. The dashed curve in Fig. 11a is the damping calculated from formula (4.13). Some discrepancy between experiment and calculation is possibly due to the fact that a definite contribution to the temperature dependence of the damping can be made by the point defects produced in reduced crystals.

Investigations of the electron-phonon interactions are of great interest, particularly since the character of these interactions can be controlled with an external electric field. Thus, if the carrier drift velocity in the external field exceeds the propagation velocity of the elastic waves, then the latter are not attenuated but are amplified[52]. Of considerable interest are also other effects connected with electron-phonon interaction, for example acoustoelectric effects and nonlinear interactions. These questions are considered in the reviews[45b,53].

c) Scattering by defects. A real crystal always contains defects or of one kind or another, which can affect the damping of the elastic waves. In principle, defects of any size can scatter elastic waves directly, thereby increasing their damping. However, an appreciable contribution to the total damping should be expected only in scattering of elastic waves by defects having dimensions close to the elastic-oscillation wavelength[31b]. Since the wavelength is on the average 0.5 μ even at 10^{10} Hz, a noticeable additional damping will be caused by defects having macroscopic dimensions. Such defects can be pores, inclusions of a foreign phase, etc. Scattering by such defects is considered, for example, in[54].

Point defects in a crystal (impurities, vacancies, interstitial atoms) are defects of atomic scale. The dimensions of these defects, even when account is taken of the strong crystal-lattice distortion produced by them, do not exceed several dozen Angstrom, i.e., they are much smaller than the wavelength. Consequently direct scattering of elastic waves by such defects makes a negligible contribution to the total damping[31b]. Nonetheless, point defects can affect the damping of elastic waves, by acting on them via thermal phonons. As already noted, damping both by the Akhiezer mechanism and by the Landau-Rumer mechanism is determined by the thermal-phonon relation time. In crystals with point defects, the relaxation time decreases, owing to scattering of the thermal phonons by the defects. This should cause a corresponding change in the damping. Thus, in the case of the Akhiezer mechanism, according to (4.5), a decrease in the relaxation time (a decrease in the thermal conductivity) in a crystal with point defects should cause a similar decrease in the damping. It was indeed observed in a number of studies that the damping of elastic waves in crystals with defects is smaller than the damping in pure crystals. It was shown in[21a] that in silicon crystals with 5×10^{17} cm^{-3} of oxygen, the damping of the longitudinal wave is decreased by approximately 10% at 100°K in comparison with silicon containing less than 10^{15} cm^{-3}

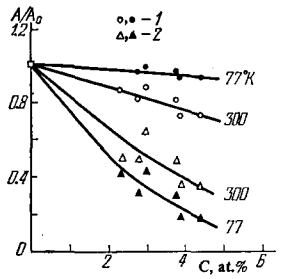

FIG. 12. Relative decrease of the damping of 1000-MHz elastic waves in silicon vs the germanium impurity concentration for longitudinal (1) and transverse (2) waves.

of oxygen. A small decrease in the damping of longitudinal waves was observed in quartz bombarded with neutrons[55] and in the germanium-silicon system in comparison with pure germanium and silicon[56]. The effect of an impurity on the damping of elastic waves was investigated in greater detail in[57] for silicon crystals doped with germanium. The results of this study are illustrated in Fig. 12, which shows the dependence of the relative decrease of the damping of the elastic waves on the concentration of the germanium impurity in the silicon. For longitudinal waves, the effect is negligible, and the damping at room temperature decreases approximately 20% at a germanium concentration of about 4 at.%. For transverse waves, the damping changes more strongly, and at the same germanium concentration the damping is decreased by an approximate factor 3 at room temperature and by a factor 5–6 at liquid-nitrogen temperatures. Measurements show[57] that in silicon crystals with 4 at.% germanium the thermal conductivity is approximately one-tenth that of pure silicon at room temperature, and one-thirtieth at liquid-nitrogen temperature. According to (4.5) this decrease of the thermal conductivity should cause a similar decrease in the damping, but this contradicts the experimental results.

The question of the influence of impurities on the damping of elastic waves was considered theoretically in[3ib], where it was shown that in the calculation of the damping of elastic waves in crystals with impurities one cannot simply replace the thermal-phonon relaxation time in the pure crystal by the phonon relaxation time due to their scattering by the impurities. The reason is that the strong frequency dependence causes the relaxation time in scattering by impurities to increase strongly when the wave vector of the thermal phonon decreases, and this leads to a divergence if the elastic-wave damping is rigorously and consistently calculated. For long-wave thermal phonons, the phonon-phonon interactions may turn out to be more appreciable than scattering by impurities, and this must be taken into account in a quantitative analysis of the influence of the impurity on the elastic-wave damping[3ib].

The question of damping in crystals with impurities was considered in greater detail also in[58], where the Akhiezer relaxation in crystals with impurities was represented in the form of two successive stages. First, the elastic scattering by defects causes phonons of different modes but of equal frequency to relax to a certain effective temperature. The phonon-phonon interactions then cause relaxation of all the phonon modes to a common average temperature. It is shown in the paper that the influence of the impurities on the damping depends strongly on the polarization and on the propagation direction of the elastic waves, on the temperature, and on the anharmonicity constant. One of the conclusions of the paper is that for transverse waves the influence of the impurities may turn out to be stronger than for longitudinal waves, a fact that agrees qualitatively with the results of[57].

In addition to the influence exerted via the thermal phonons, the point defects can also directly affect the damping of elastic waves. This occurs when a point defect has several equilibrium positions in the lattice, but these positions become non-equivalent under the influence of the deformations in the elastic wave. For elastic waves, a relaxation peak of absorption will then be observed, with a maximum corresponding to the condition $\Omega = \omega_0 \exp(-U/kT)$, where ω_0 is the characteristic frequency and U is the activation energy for the jumping of the defect from one position to another. A study of the dependence of the absorption peaks on the propagation direction and polarization of the elastic waves can yield information on the nature of the defects.

Relaxation absorption peaks for transverse elastic waves were observed[50] in lithium-niobate crystals with defects (Fig. 13). The defects were produced in these crystals by annealing in a reducing atmosphere. The activation energy determined from the frequency shifts, and also from the widths and shapes of the relaxation peaks was found to be 0.25 eV. This activation energy is apparently connected with the motion of the lithium ions in the lattice.

Another example of absorption relaxation peaks is illustrated in Fig. 14, which shows the temperature dependence of the damping of the elastic waves in NaF crystals irradiated with γ rays from Cu^{60}. The activation energy for the motion of defects turns out to be 0.04 eV in this case. Absorption peaks connected with defects were observed also in quartz after bombardment with neutrons[55], and in reduced rutile crystals[59].

We note in conclusion that the damping of elastic waves can also be affected by dislocations, but the dislocations have apparently a much smaller effect at hypersonic frequencies than in the ultrasonic band[60].

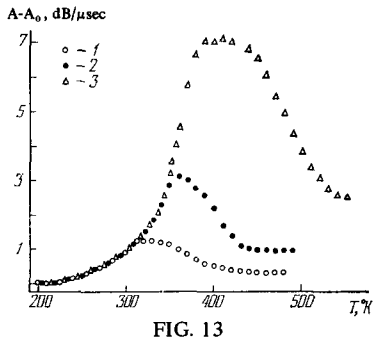

FIG. 13

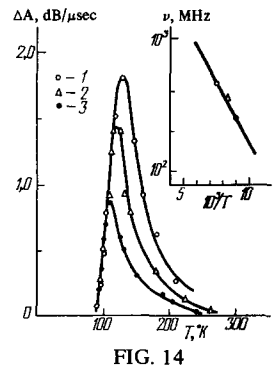

FIG. 14

FIG. 13. Relaxation peaks of absorption of transverse elastic waves propagating along a threefold axis in $LiNbO_3$ crystals reduced in an atmosphere of argon with a partial oxygen pressure 10^{-6} atm at frequencies 80 (1), 200 (2), and 500 MHz (3).

FIG. 14. Relaxation peaks of absorption of longitudinal elastic waves in the propagation along [110] in γ-irradiated NaF cyrstals at frequencies 460 (1), 350 (2), and 260 MHz (3).

5. FEATURES OF PROPAGATION OF HYPERSONIC WAVES IN MAGNETICALLY ORDERED CRYSTALS

The propagation of hypersonic waves in magnetically ordered crystals is accompanied by singularities connected with the direction of these waves with the spin waves. These singularities will be considered in the present chapter with cubic yttrium iron garnet crystals as examples.

Spin waves, i.e., magnetization oscillations propagating through the crystals, are characterized by the following dispersion relations[61a,62]

$$\omega_c = \gamma\,[(H + Dq^2)\,(H + 4\pi M_0 \sin^2\theta + Dq^2)]^{1/2}; \qquad (5.1)$$

where γ is the gyromagnetic ratio, M_0 is the saturation magnetization, D is the exchange constant, θ is the angle between the magnetization and the propagation direction of the spin waves, and $H = H_0 + H_a + H_d$, is the internal field (H_0, H_a, and H_d are the external field, the anisotropy field, and the demagnetizing field, respectively).

In the general case there exists between the elastic and spin waves a coupling that becomes particularly strong under resonance conditions, when the frequencies and wave vectors of the elastic and spin waves are equal[61a]. If we write down the dispersion equation for the elastic waves in the form $\omega = vq$, then we can easily find these conditions. Thus, at $\theta = 0^\circ$ and in the absence of the external field we have $\omega = \omega_c = \gamma(H_a + Dg^2)$, which yields two values of the resonant frequencies, $\omega_1 = \gamma H_a$ and $\omega_2 = v^2/\gamma D$, at which "crossing" of the dispersion characteristics of the spin and elastic waves takes place. Let us estimate these frequencies for an yttrium iron garnet. Using the values $H_a \approx 100$ Oe, $D = 5 \times 10^{-9}$ Oe-cm^2 and $v \approx 5 \times 10^5$ cm/sec, we obtain $\omega_1/2\pi \approx 3 \times 10^8$ Hz and $\omega_2/2\pi \approx 5 \times 10^{11}$ Hz.

In the general case of arbitrary θ, the frequency ω_2 remains practically unchanged, and

$$\omega_1 = \gamma\,[H_a\,(H_a + 4\pi M_0 \sin^2 0)]^{1/2}. \qquad (5.2)$$

The largest value of ω_1 is obtained at $\theta = 90^\circ$ and for yttrium iron garnet ($4\pi M_0 \approx 1800$ Oe) it amounts to $\omega_1/2\pi \approx 10^9$ Hz.

Figure 15 shows the dispersion characteristics of spin and elastic waves as well as the "crossing" points (in fact, in the presence of interaction, a repulsion of the spectra occurs at the "crossing" points, as is indeed seen from the figure; the dashed curves correspond to the absence of interaction.

The frequency ω_2 lies in a region not accessible to experiment at present, but ω_1 lies in a convenient frequency band. We note that the existence of a

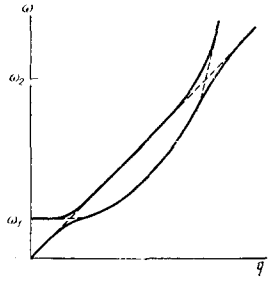

FIG. 15. Dispersion characteristics of spin and elastic waves.

"crossing" point at a frequency ω_1 in the absence of an external magnetic field is connected with the spin-wave spectrum gap due to the magnetic-anisotropy fields. The spin-wave frequency depends, according to (5.1), on the external magnetic field, and this dependence is particularly strong at frequencies where the term Dq^2 can be neglected (this corresponds to the usual experimental conditions). Then, at a given elastic-wave frequency ω, the resonance condition are satisfied in an external field

$$H_0 = 2\pi M_0\,\{[4\,(\omega^2/\omega_M^2) + \sin^4\theta]^{1/2} - \sin^2\theta\} - (H_d + H_a), \qquad (5.3)$$

where $\omega M = 4\pi\gamma M_0$. For spherical yttrium iron garnet samples ($H_d = -4\pi M_0/3$) at 10^3 MHz we obtain for the resonance field $H_0 \approx 1000$ Oe at $\theta = 0^\circ$ and $H_0 \approx 700$ Oe at $\theta = 90^\circ$.

So far we have considered fields and frequencies at which the resonance conditions for the interaction of elastic and spin waves are satisfied. For such an interaction to take place, however, it is necessary that a coupling exist between these waves. The question of the coupling can be explained by obtaining the equation of motion for the elastic displacements and the magnetization. The equations of motion are derived from the expression for the total energy E of the crystal[7]

$$\ddot{\rho u}_i = \frac{\partial}{\partial r_k}\left(\frac{1+\delta_{ik}}{2}\,\frac{\partial E}{\partial \varepsilon_{ik}}\right), \quad \dot{\boldsymbol{\alpha}} = \frac{\gamma}{M}\,[\boldsymbol{\alpha}\times\nabla_\alpha E]; \qquad (5.4)$$

Here $\boldsymbol{\alpha}$ is a unit vector along the magnetization direction. The total crystal energy is given approximately by

$$E = E_Z + E_E + E_{ME},$$

where E_Z, E_E, and E_{ME} are the Zeeman, elastic, and magnetoelastic energies, equal to

$$E_Z = -M_0\,(\alpha_i H_i), \quad E_E = c_{ijkl}\varepsilon_{ij}\varepsilon_{kl}/2, \quad E_{ME} = b_{ijkl}\alpha_i\alpha_j\varepsilon_{kl}. \qquad (5.5)$$

The expression for the energy includes neither the exchange energy, since its contribution is small at the customarily employed frequencies, nor the magnetic-anisotropy energy, since it leads to a change of the resonant frequency in the considered approximation.

For cubic crystals, the expression for the energy contains two independent magnetoelastic coefficients[17], which are customarily introduced in the following manner: $b_{11} - b_{12} = B_1$ and $2b_{44} = B_2$. When these coefficients are used, we obtain

$$E_{ME} = B_1\alpha_i^2\varepsilon_{ii} + \beta_2\alpha_i\alpha_k\varepsilon_{ik}\,(1-\delta_{ik}).$$

In the derivation of the equations of motion it is assumed that all the perturbations are small, i.e., only terms of first order relative to the variable displacements and magnetization are retained in the equations of motion. The solution of these equations is sought in the form of plane waves, and the natural frequencies and the dispersion relations are obtained by setting equal to zero the determinant of the system of homogeneous equations for the plane-wave amplitudes. Such a problem was solved in[63] for the case of elastic and magnetoelastic isotropy and for an arbitrary direction of propagation relative to the magnetic field. A solution is given in[64] for different directions of propagation of the elastic waves relative to the crystallographic axes and to the magnetic field in a cubic crystal.

Let us consider a case in which the elastic wave propagates along the [100] direction (x axis), and the magnetic field lies in the (010) plane (the x, z plane). Using (5.4) and (5.5), and also Maxwell's equations for the alternating[61a] magnetization **M** and magnetic field **h** (curl **h** = 0 and div **h** = -4π div **M**), we obtain an equation for the amplitudes of the plane waves:

$$\left.\begin{aligned} i\omega M'_x + \gamma H M'_y - i\gamma B_2 q\cos\theta\cdot u_y = 0,\\ \gamma(H+4\pi M_0\sin^2\theta)M'_x - i\omega M'_y + i\gamma B_2 q\cos 2\theta\cdot u_z - i\gamma B_1 q\sin 2\theta\cdot u_x = 0,\\ (iB_2q/\rho M_0)\cos 2\theta\cdot M'_x + (\omega^2 - v_S^2q^2)u_z = 0,\\ (iB_2q/\rho M_0)\cos\theta\cdot M'_y - (\omega^2 - v_S^2q^2)u_y = 0,\\ (iB_1q/\rho M_0)\sin 2\theta\cdot M'_x - (\omega^2 - v_L^2q^2)u_x = 0; \end{aligned}\right\} \quad (5.6)$$

here $v_S = (c_{44}/\rho)^{1/2}$ and $v_L = (c_{11}/\rho)^{1/2}$ are the velocities of the transverse and longitudinal waves, while the coordinate system x'yz' is connected with the field H, which is directed along the z' axis.

In the case $\theta = 0$, i.e., when the magnetic field is parallel to the propagation direction, we seek the solutions in the form of circularly-polarized plane waves $M^{\pm} = M_y \pm iM_z$ and $u^{\pm} = u_y \pm iu_z$. It then follows from (5.6) that

$$(\omega \mp \omega_0)M^{\pm} \pm i\gamma B_2 q u^{\pm} = 0, \quad (B_2q/\rho M_0)M^{\pm} + i(\omega^2 - v_S^2q^2)u^{\pm} = 0,$$

where $\omega_0 = \gamma H$ is the resonant frequency for the case $\theta = 0$. From the vanishing of the determinant of this system we obtain the dispersion relation

$$(\omega \mp \omega_0)(\omega^2 - v_S^2q^2) \mp (\gamma B_2^2 q/\rho M_0) = 0,$$

which yields two solutions

$$(q^{\pm})^2 = \omega^2\{v_S^2 - [\gamma B_2/\rho M_0(\omega_0 \mp \omega)]\}^{-1}. \quad (5.7)$$

Thus, one of the circularly-polarized components of the elastic wave (u^-) is practically not coupled with the spin waves.

Let us examine in greater detail the dispersion relation for the component u^+ which is coupled with the spin waves:

$$(\omega - \omega_0)(\omega^2 - v_S^2q^2) - (\gamma B_2^2 q^2/\rho M_0) = 0.$$

Since $\omega + v_S q \approx 2\omega_0$ in the resonance region, we obtain

$$\omega_{1,2} = 0.5(\omega_0 + v_S q) \pm 0.5[(\omega_0 - v_S q)^2 + (2\gamma B_2^2\omega_0/\rho M_0 v_S^2)]^{1/2},$$

i.e., as already noted, a repulsion of the dispersion curves occurs in the resonance region. The splitting of the two branches $\Delta\omega = \omega_1 - \omega_2$ is minimal at $\omega_0 = v_S q$ (the "crossing" point) and is equal to $\Delta\omega = (2\gamma B_2^2\omega_0/\rho M_0 v_S)^{1/2}$.

Let us examine, further, the case $\theta = 90°$, when the magnetic field is perpendicular to the elastic propagation direction. In this case, as follows from (5.6), the transverse waves with polarization perpendicular to the direction of the magnetic field turn out to be not coupled with the spin waves $q_1^2 = \omega^2/v_S^2$. For the coupled waves we obtain

$$(\omega^2 - v_S^2q_2^2)(\omega_0^2 - \omega^2) + (B_2^2\gamma^2 H q_2^2/\rho M_0) = 0.$$

Hence

$$q_2^2 = \omega^2/\{v_S^2 - [B_2^2\gamma^2 H/\rho M_0(\omega_0^2 - \omega^2)]\}; \quad (5.8)$$

here ω_0 is the resonance frequency at $\theta = 90°$, i.e.,

$$\omega_0 = \gamma[H(H + 4\pi M_0)]^{1/2}.$$

It also follows from (5.6) that longitudinal elastic waves are not coupled with the spin waves at $\theta = 0$ and 90°. At other values of θ, the coupling does exist and becomes maximal at $\theta = 45°$.

We can determine in similar fashion also the coupling of spin waves with elastic waves propagating in other directions. We present the results for some of the most interesting cases[64]. For propagation along the [110] direction in a field perpendicular to the propagation direction, the longitudinal waves turn out to be coupled with the spin waves, and the coupling constant is given by the expression$((B_1 - B_2)\sin 2\beta$, where β is the angle between the direction of the field and the [001] direction. It is interesting to note that a coupling exists in this case in the presence of magnetoelastic isotropy, when $(b_{11} - b_{12})/b_{44} = 1$, i.e., $B_1 = B_2$. For propagation along ⟨111⟩ in a field parallel to the propagation direction, the normal modes are, just as in the case of ⟨100⟩, waves with circular polarization. The dispersion relation turns out to be the same as (5.7), but the coupling is described by an effective magnetoelastic constant equal to $(2B_1 + B_2)/3$. The longitudinal waves do not interact with the spin waves in this case.

Transverse waves propagating along [110] in a field parallel to [110] are connected with the spin waves, and the coupling turns out to be different for waves with polarization along the $[1\bar{1}0]$ and [001] directions. When the field is perpendicular to the propagation direction, a coupling exists for transverse waves with polarization along $[1\bar{1}0]$ and [001] if the magnetic field is directed along the respective directions.

After the publication of the first theoretical papers on magnetoelastic interaction[61b], detailed experimental studies were made of the interaction of elastic waves with spin waves, principally with yttrium iron garnet crystals as examples[24a,64-66,67a,68-72]. These investigations have shown that the predictions of the theory of magnetoelastic interaction agree well with experiment.

Let us examine some of the experimental results. In[69,71], in an investigation of the propagation of elastic waves with frequencies 100–1700 MHz in yttrium iron garnet crystals in the absence of an external magnetic field, sharp damping peaks were observed (Fig. 16), the frequencies of which depended on the propagation direction. An investigation of the dependence of these

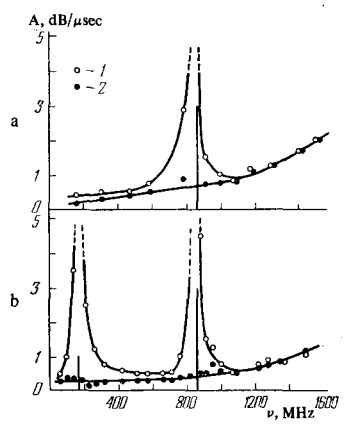

FIG. 16. Natural magnetoelastic resonance in the propagation of longitudinal (a) and transverse (b) elastic waves along the [111] direction in yttrium iron garnet crystals at H = 0 (1) and 4000 Oe (2).

peaks on the temperature and on the external magnetic field has shown that they are of magnetic origin. Since the frequencies at which the damping peaks were observed fall in the range defined by formula (5.2), the following explanation was proposed for the results[69,71]:

The damping peaks are connected with the resonant magnetoelastic interaction, and to calculate the resonance frequency it is necessary to use formula (5.2) with allowance for the fact that in the absence of an external magnetic field the sample consists of magnetic domains. If it is assumed that the magnetization of the majority of the domains is directed along the easy-magnetization directions ⟨111⟩, it is necessary to substitute for the angle θ in (5.2) all the possible angles between directions of the ⟨111⟩ type and the propagation direction of the elastic waves, and it is necessary to choose for the anisotropy field the values for the ⟨111⟩ direction i.e., $H_a = 4K_1/3M_0$, where K_1 is the anisotropy constant. Thus, for propagation along ⟨111⟩ there exist two possible angles θ, 0° and 70°3.2′. According to (5.2), this leads to the resonant frequencies 170 and 870 MHz, respectively. As seen from Fig. 16, it is precisely at these frequencies that the absorption peaks are observed. We note that no low-frequency peak is observed for longitudinal waves because, as noted above, the longitudinal waves are not coupled with the spin waves in the case of propagation along ⟨111⟩ at $\theta = 0°$. Good agreement between calculation and experiment was observed also for other propagation directions, thus confirming the validity of the proposed model (see Table II, which gives the frequencies of the natural magnetoelastic resonance for yttrium iron garnet crystals).

By analogy with natural ferromagnetic resonance, the resonant absorption of elastic waves in the absence of an external magnetic field can be called natural magnetoelastic resonance, since this resonance occurs in equivalent magnetocrystallographic anisotropy fields. It should be noted that a similar phenomenon was observed in[24a], where the temperature dependence of the damping of longitudinal 1000-MHz waves was measured. Damping peaks were observed at a temperature close to 250°K. These results agree with the temperature dependence obtained in[69] for the resonant frequencies at higher temperatures. The authors of[24a] have drawn, however, the erroneous conclusion that the damping peaks are connected with interactions between elastic waves and magnetic-domain walls.

Magnetoelastic resonance in yttrium iron garnet in external magnetic fields was observed in[64,66,67a,68]. It

Table II

Elastic-wave propagation direction	θ	Resonance frequency, MHz	
		Calculation	experiment
[100]	54°44′	760	750
[111]	0°	170	180
	70°32′	870	850
[1$\bar{1}$0]	35°16′	550	550
	90°	930	940
[113]	30°	490	470
	58°	790	750
	80°	910	900

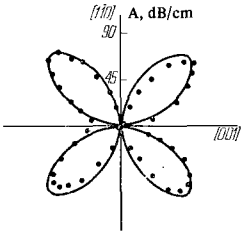

FIG. 17. Polar diagram of the damping of longitudinal elastic waves in magnetoelastic resonance vs the angle β between the magnetic field and the [001] direction for an yttrium iron garnet crystal.

was shown in[64] that the character of the interaction of the elastic waves with the spin waves is well described by the phenomenological theory of magnetoelastic interaction. Thus, for longitudinal waves propagating along ⟨100⟩, there is no resonance in a field parallel or perpendicular to the propagation direction, as is indeed called for by the theory. In the propagation of longitudinal waves along ⟨110⟩, and in a field perpendicular to the propagation direction, a resonance is observed and its depth depends on the field direction relative to the crystal axis (see Fig. 17, where the elastic waves propagate perpendicular to the field along the [1$\bar{1}$0] direction, the frequency is 1470 MHz, and the solid line is drawn under the assumption that the damping is proportional to $\sin^2 2\beta$). As indicated above, the connection between the elastic and spin waves is determined in this case by a constant proportional to $(B_1 - B_2)\sin 2$, where β is the angle between the direction of the field and the [110] direction. It follows from Fig. 17 that the experiment agrees well with the theory (the sample used in these measurements was a thin plate). We note also that the value of the field at which the resonances are observed coincides with the value calculated from formula (5.3).

For transverse elastic waves one observes, in addition to resonant damping, also effects connected with the differences of the interaction of different displacement components in the elastic wave with the spin waves. In propagation along ⟨100⟩ or ⟨111⟩ in a field parallel to the propagation direction, the normal modes are circularly-polarized waves with opposite directions of rotation. One of them interacts with the spin wave, and this leads to a change in the propagation velocity, while the other is practically non-interacting.

In experiments with elastic waves, it is customary to use converters that excite and register linearly-polarized transverse waves with definite polarization direction.

A linearly polarized wave from an input converter that acts thus as a polarizer is resolved in the crystal into two circularly-polarized components that propagate with different velocities. For the resultant linearly-polarized wave in the output converter (or in the input converter when working "in reflection") the polarization plane is rotated through a certain angle φl (l is the path traversed by the elastic wave) relative to the initial plane. The receiving converter, which serves as the analyzer, generates a signal proportional to $\cos(\varphi l)$. Since the change in the velocity of the interacting component depends on the field, the angle will change with changing field, and with it the amplitude of the signal in the receiving converter. The signal has a maximum value at $\varphi l = n\pi$, where n = 0, 1, 2, . . . , and a minimum value at $\varphi l = (2n + 1)\pi/2$. Thus, as the field changes, the elastic-pulse amplitude

registered by the receiving converter oscillates. Such oscillations should be observed not only when the field changes, but also in a constant field if a series of successive elastic pulses are obtained as a result of multiple reflections from the ends of the sample. The oscillations are connected in this case with the fact that each succeeding pulse in the series traverses a longer total path through the sample and its plane of polarization is rotated through a larger angle. Since $\varphi = (q^+ - q^-)/2$, we obtain from (5.7)

$$\varphi = (\pi B^2\nu^2/M_0\rho\gamma v_S^3)/[H^2 - (\nu/\gamma)^2],$$

where γ = 2.8 MHz/Oe, and B is equal to B_2 when the elastic waves propagate along ⟨100⟩ and to $(2B_1 + B_2)/3$ in the case of propagation along ⟨111⟩.

The above-described rotation of the polarization plane, which can be called the acoustic Faraday effect, was observed first in[65] in cylindrical yttrium iron garnet samples at 500 MHz. The Faraday effect was investigated in[70] at 9×10^9 Hz, and in[72] under conditions of a homogeneous internal magnetic field (spherical sample). The experimental results obtained in the indicated studies agree well with the theory. In[64] we have also confirmed by direct experiment that only one circularly-polarized component of the elastic waves, with a definite direction of rotation, interacts with the spin waves. A circularly polarized elastic wave was produced by the method of quarter-wave plates[14]. These were yttrium aluminum garnet plates[73] approximately 0.5 mm thick, cut perpendicular to the ⟨110⟩ direction. At definite elastic-wave frequencies, the plate operates like a quarter-wave plate and converts the linearly-polarized wave produced by the input converter into a circularly-polarized wave. The result of the experiment is given in Fig. 18, which shows the dependence of the transverse elastic-wave pulse amplitude on the magnetic field at two frequencies. The resultant wave entering the yttrium iron garnet sample is linearly polarized at one frequency, 1340 MHz (Fig. 18a), and circularly polarized at the other frequency, 1500 MHz (Fig. 18b). In Fig. 18, I and II denote the results for a field parallel and antiparallel to the propagation direction; 1, 2, and 3 denote the sample, the piezoconverter, and the yttrium aluminum garnet plate. As seen from Fig. 18, oscillation of the pulses is observed in the former case (the acoustic Faraday effect), but in the second case there are practically no such oscillations, only a decrease of the pulse amplitude at resonance. Reversal of the field direction changes the spin-precession direction. For the linearly-polarized wave one observes then, as before, oscillation of the pulses, while the amplitude of the pulses of the circularly polarized wave ceases to depend on the field. This experiment shows that the spin waves, indeed, interact only with the circularly polarized elastic wave with a rotation direction determined by the direction of the spin precession and the magnetic field.

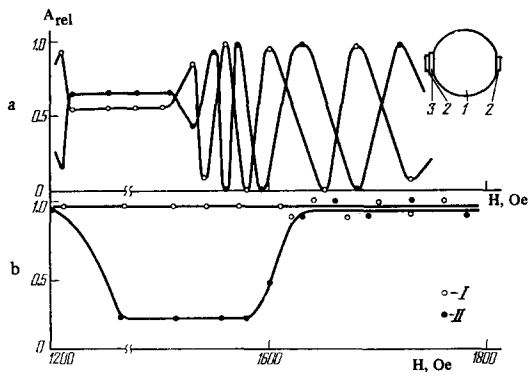

FIG. 18. Amplitudes of transverse elastic-wave pulses in propagation along [100], vs the magnetic field for yttrium iron garnet.

Oscillations of pulses of transverse elastic waves are observed also in other cases[64], for example in propagation along ⟨100⟩ for a field perpendicular to the propagation direction, and in propagation along ⟨110⟩ for both parallel and perpendicular fields. In these cases the oscillations are connected with the fact that the simultaneously excited linearly-polarized waves with two possible polarization directions interact differently with the spin waves. This is thus a birefringence effect.

Figure 19 shows the dependence of the transverse elastic-wave pulse amplitude on the magnetic field in propagation along ⟨100⟩ perpendicular to the field. The polarization direction of the elastic waves makes an angle 45° with the field direction (frequency 1580 MHz; 1 and 2 denote the first and second pulses, respectively; the region of very fast oscillations is shaded). Waves with polarization parallel and perpendicular to the field are excited simultaneously. For the specific phase-shift angle between the components $\varphi = q_1 - q_2$ we obtain from (5.8)

$$\varphi = (\pi B_2^2\nu/M_0\rho v_S^3)\, H/[H\,(H + 4\pi M_0) - (\nu/\gamma)^2].$$

This formula describes well the results shown in Fig. 19.

The interaction of elastic waves with spin waves was investigated mainly and for the most part in yttrium iron garnet crystals. Magnetoelastic interaction was investigated also in a few other crystals with garnet structure[67b,68,74]. Effects of acoustic birefringence in magnetite and nickel crystals were observed in[67c].

6. LIGHT SCATTERING BY HYPERSONIC WAVES

A survey of hypersonic waves would be incomplete without a consideration of the scattering of light, which

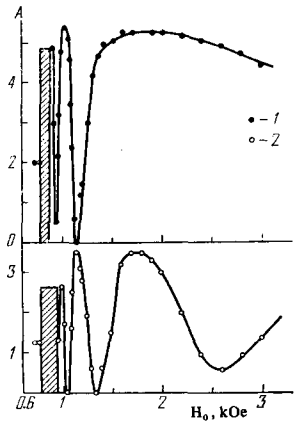

FIG. 19. Amplitude of transverse elastic wave pulses vs the magnetic field for propagation along ⟨100⟩ perpendicular to the magnetic field.

is a precise tool for the investigation of the elastic-wave propagation characteristics[75] and makes it possible, in addition, to investigate elastic waves at high frequencies at not too low temperatures. The scattering of light by elastic waves is a sufficiently broad and interesting problem, which could easily be the topic of a separate review. We consider only very briefly the most important features of the phenomenon, and also its use for the investigation of hypersonic waves.

As shown by Rytov[76], two limiting cases are distinguished when light interacts with elastic waves. If the wavelength Λ of the elastic oscillations is sufficiently large, so that the condition $\Lambda^2/\lambda > l$ is satisfied where λ is the wavelength of the light in the medium and l is the width of the beam of the elastic waves in the propagation direction of the light, then the so-called Raman-Natov diffraction takes place. After passing through the crystal, the light splits into many orders separated by an angle λ/Λ. In the other limiting case, when $\Lambda^2/\lambda < l$, which takes place at high elastic-wave frequencies, only the first order is observed in the diffraction pattern, and the diffraction of the light occurs only if the light is incident at a definite angle to the front of the elastic wave. This case is called Bragg diffraction. At the usually experimental values $l \lesssim 1$ cm for hypersonic waves ($\nu > 10^8$ Hz), the Bragg diffraction conditions are satisfied. To determine the scattering geometry in this case one can use the energy and momentum conservation laws[75]:

$$\omega_2 = \omega_1 \pm \Omega, \quad \mathbf{k}_2 = \mathbf{k}_1 \pm \mathbf{q}; \tag{6.1}$$

here ω and $\mathbf{k}$ are the frequency and wave vector of the light, Ω and $\mathbf{q}$ are the frequency and wave vector of the elastic waves, and the subscripts 1 and 2 pertain to the incident and reflected light, respectively, From the energy conservation law we obtain $k_2 = k_1[1 \pm (\Omega/\omega_1)]$, and since $\Omega \ll \omega$, it follows that $k_2 \approx k_1$, i.e., the vector triangle (Fig. 20a) representing the momentum conservation law is isosceles. From this triangle we obtain $\theta_1 = \theta_2 = \theta_B$ and $\sin\theta_B = q/2k$, or, in terms of frequency,

$$\sin\theta_B = (\Omega/2\pi)(\lambda_0/2n\nu) = \nu\lambda_0/2n\nu, \tag{6.2}$$

where n is the refractive index and v is the velocity of the elastic waves. The incidence and diffraction angles θ_1 and θ_2 are reckoned from the normal to the vector $\mathbf{q}$, i.e., from the wave front of the elastic wave, and in the case of the geometry of Fig. 20a they are taken to be positive. Thus, scattering of light by elastic waves occurs if the light is incident at an angle θ_B relative to the front of the elastic wave. The scattered (diffracted) light makes in this case an angle θ_B with the front, so that the total scattering angle is $2\theta_B$. The geometry and the experimental setup on the scattering of light by elastic waves are shown in Fig. 21.

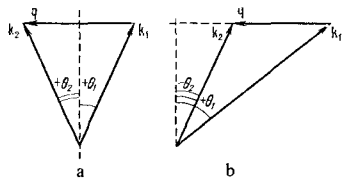

FIG. 20. Law of momentum conservation in ordinary Bragg scattering of light (a) and in scattering with rotation of the plane of polarization in an optically unisotropic crystal (b).

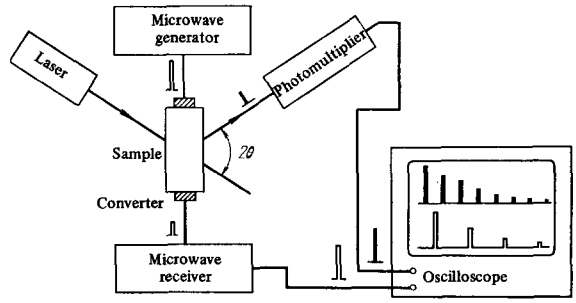

FIG. 21. Setup for experiments on the scattering of light by hypersonic waves.

Formula (6.2) and Fig. 20a correspond to the ordinary Bragg condition for the scattering of light in an optically isotropic medium or in an anisotropic medium when scattering is not accompanied by rotation of the plane of polarization of the light. Scattering of light by elastic waves in a crystal can, however, be accompanied by rotation of the plane of polarization of the incident light[75]. In such a case, the refractive indices for the incident and scattered light in an optically anisotropic medium turn out to be different, with $k_1 = 2\pi n_1/\lambda_0 \neq k_2 = 2\pi n_2/\lambda_0$, and the momentum vector triangle ceases to be isosceles (Fig. 20b). This leads to unique effects in the scattering of light. Such effects were investigated in[77] for the case of uniaxial crystals. From the triangle in Fig. 20b it follows that

$$\begin{aligned}\sin\theta_1 &= (\lambda_0\nu/2\nu n_1)[1 + (\nu/\lambda_0\nu)^2(n_1^2 - n_2^2)],\\ \sin\theta_2 &= (\lambda_0\nu/2\nu n_2)[1 - (\nu/\lambda_0\nu)^2(n_1^2 - n_2^2)].\end{aligned} \tag{6.3}$$

Definitions are introduced for the signs of the angles in order to emphasize the difference from the ordinary Bragg scattering (Fig. 20a). Formula (6.3) shows that the angles θ_1 and θ_2 differ from each other and depend on the elastic-wave frequency in a manner different from ordinary conditions (6.2).

Although formulas (6.3) are indeed the most general formulas (they go over into (6.2) when $n_1 = n_2$), they are convenient for use only if the scattering is in the (x, y) plane perpendicular to the optical axis of the crystal. In this case the refractive indices are equal to n_0 and n_e and do not depend on the direction of the incidence and scattered light. In the case of scattering in an arbitrary plane, the refractive index becomes a function of the angles θ_1 and θ_2, and it is therefore more convenient to analyze the singularities of the scattering geometry by using the wave-vector surface[7b], the radius vector of which determines the value of the wave vector of light propagating in a given direction. In uniaxial crystals, this is a double-cavity surface consisting of a sphere and an ellipsoid of revolution which are tangent to each other at two points on the k_z axis[7b]. To determine the possible scattering geometry and its dependence on the frequency of the elastic waves, it is necessary to take the interaction of the wave-vector surface with the scattering plane and to construct in this intersection all the possible vector triangles expressing the momentum conservation law (6.1). Such an analysis shows (see, for example, Fig. 22) that scattering of light with rotation of the plane of polarization in uniaxial crystals is characterized by a number of singularities[77].

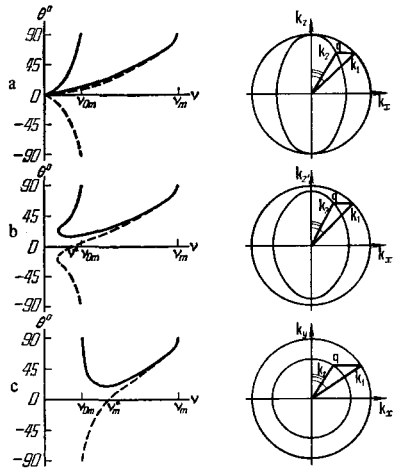

FIG. 22. Intersections of the wave-vector surface with the scattering plane, and schematic dependence of the angle θ_1 (solid line) and θ_2 (dashed) on the elastic-wave frequency.

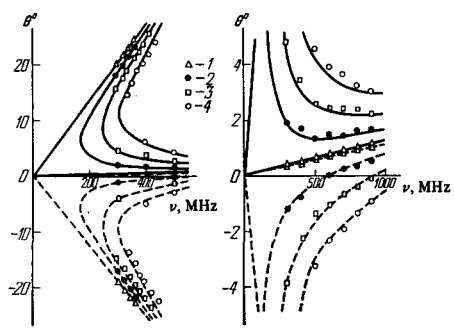

FIG. 23. The angles θ vs the frequencies of the longitudinal elastic waves propagating along the x axis in an $LiNbO_3$ crystal.

(In Fig. 22, at q ∥ x, the scattering plane is (z′, x); the z′ axis makes an angle $\alpha = 0$ (scattering plane (z, x); Fig. a), $0 < \alpha < 45°$ (b), and $\alpha = 90°$ (c) (scattering plane (y, x)).)

At a definite elastic-wave frequency ν_0, a collinear interaction is possible, in which the wave vectors of the elastic waves and of the incident and scattered light are parallel. There exists a frequency ν^* at which one of the angles, θ_1 or θ_2, is equal to zero. In the case of scattering in definite crystallographic planes, two scattering geometries are possible in certain frequency bands, i.e., two possible incidence angles θ_1 and correspondingly two diffraction angles θ_2 exist at a given frequency. The frequencies ν_0 and ν^* depend on the propagation directions of the light and of the elastic waves, and their maximum values are, respectively,

$$\nu_{0\,\max} = (v/\lambda_0)(n_0 - n_e) \text{ and } \nu^*_{\max} = (v/\lambda_0)(n_0^2 - n_e^2)^{1/2}.$$

Among the characteristic frequencies of elastic waves are also the back-scattering frequencies (scattering angle $\theta_1 + \theta_2 = 180°$), which are the maximum possible frequencies satisfying the conservation laws (6.1). These frequencies are equal to $\nu_{\max} = 2n_0 v/\lambda_0$ at q ∥ z and $\nu_{\max} = (v/\lambda_0)(n_0 + n_e)$ at q ⊥ z, where z is the optical axis of the crystal.

The values of the indicated characteristic elastic-wave frequencies (in MHz) in scattering of light in certain uniaxial crystals at $\lambda = 6328$ Å are listed in Table III (L, S_f, and S_S denote respectively longitudinal, fast transverse, and slow transverse waves).

Table 3

Crystal	Point group	n_0	n_e	q	Type of wave	$\nu_{0\,\max}$	$\nu^*_{\max}$	$\nu_{\max}$
$LiNbO_3$	C_{3v}	2,286	2,2	x	L	890	6428	46430
					S_f	647	4670	33744
					S_s	548	3955	28567
				z	L	0	7192	52941
					S	0	3520	25937
KH_2PO_4	D_{2d}	1,5074	1,4668	x	L	384	3290	28195
					S_f	149	1278	10945
					S_s	105	900	7703
				z	L	0	2716	23575
					S	0	1278	11094
Al_2O_3	D_{3d}	1,765	1,757	x	L	139	2916	61388
					S_f	86	1792	37720
					S_s	72	1512	31835
				z	L	0	3000	63293
					S	0	1634	34474
SiO_2	D_3	1,5426	1,5516	x	L	82	1517	28114
					S_f	72	1346	24936
					S_s	48	887	16427
				z	L	0	16672	30812
					S	0	1235	22815

The conclusions drawn concerning the singularities of the scattering of light in optically uniaxial crystals were confirmed experimentally for the crystals listed in Table III. By way of example, Fig. 23 shows the experimental dependences of the light incidence and diffraction angles on the frequency of the longitudinal waves in lithium niobate crystals. The elastic waves propagate along the x axis and the light is scattered in the (x, z′) plane, where z′ makes an angle α with the z axis ($\alpha = 0°$ (1), 5.5° (2), 7.5° (3), and 10° (4); the solid and dashed curves are calculated from formulas (6.4)).

If we consider the intersections of the wave-vector surface with the scattering plane (see Fig. 22), then we can show that in this case the dependence of the angles θ_1 and θ_2 on the frequency of the elastic waves and on the angle α should take the following form (at $n_0 > n_e$ and $k_1 > k_2$):

$$\sin\theta_1 = (\lambda_0 v/v n_0)\left\{n^2 \pm n_e\left[\left(\frac{v}{\lambda_0 v}\right)^2 (n^2 - n_e^2)(n^2 - n_0^2) + n^2\right]^{1/2}\right\}\Big/(n^2 - n_e^2),$$

$$\sin\theta_2 = \pm\{[1 - (n_0/n)^2\cos^2\theta_1]/(1 + [(n_0/n_e)^2 - (n_0/n)^2]\cos^2\theta_1)\}^{1/2}, \quad (6.4)$$

where

$$n^2 = n_0^2 n_e^2/(n_0^2\sin^2\alpha + n_e^2\cos^2\alpha).$$

It follows from Fig. 23 that the experimental plots agree well with those calculated from formulas (6.4).

So far we have discussed only the geometry of the scattering of light by elastic waves, without considering the interaction mechanism. The interaction of light with elastic waves is determined by the so-called photoelasticity, i.e., the change of the optical refractive index of the medium by the strains in the elastic waves. It is customary to relate the strain ϵ_{kl} with the variations of the dielectric tensor[10]:

$$\Delta B_{ij} = p_{ijkl}\epsilon_{kl}, \quad (6.5)$$

where the photoelasticity coefficients p_{ijkl} form a fourth-rank tensor that is symmetrical with respect to permutations within the first pair of indices (optical

indices) and within the second pair (acoustic indices). The number of independent components of the photoelasticity tensor depends on the symmetry of the crystal[10] and ranges from 36 for triclinic crystals to 4 or 3 (depending on the point group) for cubic crystals.

It was shown recently[78] that the tensor p_{ijkl} has in fact a lower symmetry and turns out to be asymmetrical with respect to the acoustic indices. The reason is that for an elastic wave propagating in an optically anisotropic crystal it is necessary to take into account in (6.5) not only the symmetrical combination ϵ_{kl} of the displacement gradients, but also their antisymmetrical combination, which describes rotation of the volume elements. The new symmetry properties predicted in[78a] for the tensor p_{ijkl} were confirmed experimentally in the case of scattering of light by thermal elastic waves in rutile[79] and calcite[80] crystals. The photoelastic effect (6.5), which leads to the scattering of light by elastic waves, is possessed by all solids without exception. In piezoelectrics, in addition, there exists an indirect photoelastic effect, which, as shown in[78b], cannot be described by a fourth-rank tensor.

We proceed now to examine the connection between the intensity of the light scattered by elastic waves with the characteristics of elastic-wave propagation and with the physical parameters of the crystal. Such a problem can be solved with the aid of Maxwell's equations or by the method of integral equations. For the relative intensity of the scattered light at small deformations in an elastic wave, we obtain[81]:

$$I/I_0 = (\pi^2/2)\,(n^6p^2/\rho v^3)\,P_a\,(l/h\lambda_0^2\cos^2\theta); \qquad (6.6)$$

here P_a is the (acoustic) power of the elastic wave, and l and h are the transverse dimensions of the beam of elastic waves, l being the dimension in the propagation direction of the light. In (6.6), p is an effective constant whose value depends on the propagation direction and polarization of the elastic waves, and also on the polarization of the incident and scattered light. It can be obtained from the usual transformation formulas for the components of a fourth-rank tensor. In the calculations it is convenient to use the formula[75]

$$p = \alpha_i\beta_j\gamma_k\varkappa_l p_{ijkl}, \qquad (6.7)$$

where α_i and β_j are the direction cosines of the polarizations of the incident and scattered light, and γ_k and κ_l are the direction cosines of the polarization and of the wave vector of the elastic waves. Formula (6.7) shows that in the general case an anisotropy of the intensity of the scattered light should be observed in the crystal. Such an anisotropy is illustrated in Fig. 24, which shows the dependence of the scattering intensity on the direction of the incidence of light for the case of longitudinal elastic waves propagating along the x axis in lithium niobate[82]; the directions of the axes y and z are such that a negative charge is produced upon compression; the polarization of the light is perpendicular (1) or parallel (2) to the elastic-wave propagation direction; the solid curves represent calculation by formula (6.6).

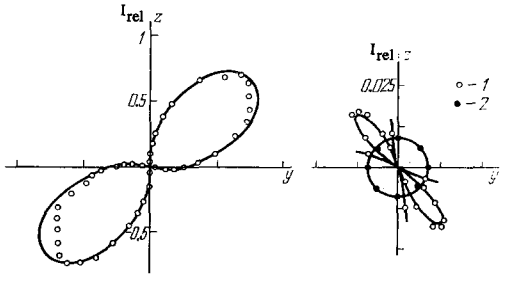

FIG. 24. Intensity of light scattering by longitudinal elastic waves propagating along the z axis vs the angle between the light incidence direction and the z axis in lithium niobate.

The question of the scattering intensity is important in hypersonic-wave experiments where the scattering of light is used to measure the propagation characteristics of these waves. The scattering intensity is determined by the physical parameters of the crystal, and namely, according to (6.6), by the quantity $n^2p^2/\rho v^3$, which can vary strongly from crystal to crystal. Among the most effective crystals for light scattering, for example, are $LiNbO_3$, $Bi_{12}GeO_{20}$, GaP, α-HIO_3 and TeO_2. At $\lambda_0 = 6328$ Å, the effectiveness of the scattering in these crystals, relative to molten quartz, is 4.6[83], 6.6[84], 30[83], 55[85], and 500[86], respectively.

In concluding this chapter, let us see how the phenomenon of light scattering can be used to investigate the propagation of hypersonic waves in crystals. Light scattering makes it possible to measure all the characteristics of hypersonic-wave propagation, and with greater sensitivity than ordinary radio methods (see Chap. 2). We note in this connection that light scattering was used to register these waves even in Baranskiĭ's first work on the excitation of hypersonic waves in quartz crystals. It follows from (6.2), (6.6), and (6.7) that by measuring the angles and intensity of the scattering we can determine the velocity and propagation direction of the elastic waves, their polarization, the direction of energy flow, and also the acoustic power of the elastic wave. From measurements of the acoustic power at two neighboring points in the crystal along the propagation direction of the elastic wave we can determine the damping.

The use of light scattering to measure damping permits the experiments to be performed at higher frequencies and temperatures than obtaining with the aid of radio methods of registration. Thus, it is easily seen that with ordinary radio methods, as a rule, it is impossible to obtain, for example, elastic waves of frequency 10^{10} Hz at room temperature. Indeed, for most crystals, the damping under such conditions amounts to 100 dB/cm and more (the Akhiezer mechanism). If the power of the electromagnetic-oscillation generator is 1 W, the crystal length is 1 cm, and the double-conversion loss is 50 dB, then the signal at the output of the receiving device will be 10^{-15} W. A good microwave receiver has a sensitivity 10^{-12} W, i.e., such a signal cannot be registered. With the aid of the light-scattering method[87], however, this becomes perfectly feasible. The high sensitivity of this method can be used also to register acoustic harmonics resulting from the anharmonicity of the interaction forces when elastic waves propagate in crystals.

Light scattering yields also other information that is frequently of interest, such as the distribution of

the acoustic power over the cross section of the crystal. This can be obtained either by measuring the scattering intensity at individual points over the cross section, or by rotating the crystal in the scattering plane about the position determined by formula (6.2). In the latter case the angular dependence of the scattering intensity is the Fourier transform of the distribution of the elastic-wave intensity over the crystal cross section.

Finally, the light scattering in itself can be used as a source of intensive hypersonic waves of high frequency. Such waves are produced, for example, in a crystal by electrostriction mixing of two laser beams that are shifted in frequency[89] or in stimulated Mandel'shtam-Brillouin scattering of light[90].

7. CONCLUSION

Investigations of crystals by hypersonic methods began approximately 10 years ago. During the elapsed time, a large number of studies were devoted to the main regularities of the propagation of hypersonic waves in crystals of various types. The main features of the interaction of hypersonic phonons with thermal phonons, magnons, free carriers, and photons were determined, and the applicability of different theoretical models was established. These studies, the principal results of which are described in this review, have shown that hypersonic methods can be used to answer many questions of interest in solid state physics, for example, the characteristics of phonon and magnon spectra (relaxation times, anharmonicity constants, dispersion relations), the parameters of electron phonon interactions, and the properties and structures of defects.

In addition to the investigations considered in the present review, the use of hypersonic waves is also promising for the investigation of the following: 1) the electronic structure of metals and alloys, including superconductors[54]; 2) nonlinear effects in the propagation of elastic waves in crystals, the study of which yields information on the anharmonicity of the interatomic interaction forces and on the phonon-phonon coupling constant[91]; 3) various aspects of the electron-phonon interactions in semiconductors[45b]; 4) effects connected with the interaction of hypersonic waves with paramagnetic ions[6]; 5) investigations of the anomalies of the propagation of elastic waves near phase transitions, which yield additional data on the mechanism of the transitions, and on the behavior of soft phonon modes; some problems connected with the latter are discussed in[92].

We indicate also that hypersonic waves can serve not only as a useful method of research in solid state physics, but finds interesting practical applications. By way of example of such applications, we can mention delay lines in microwave technology, microwave amplifiers and oscillators, and devices for the modulation and scanning of laser beams.

[1] K. H. Baranskiĭ, Dokl. Akad. Nauk SSSR 114, 517 (1957) [Sov. Phys.-Doklady 2, 237 (1958)] Kristallografiya 2, 299 (1957) [Sov. Phys.-Crystallogr. 2, 296 (1957)].

[2] J. B. Thaxter and P. E. Tannenwald, IEEE Trans. Sonics and Ultrasonics SU-13, 61 (1966).

[3] J. Ilukor and E. Jacobson; Science 153, 1113 (1966).

[4] R. J. von Gutfeld, Physical Acoustics, v. 5, ed by W. P. Mason, N. Y.-L., Academic Press, 1968, p. 233.

[5] B. Roberts, Physical Acoustics (ed. by W. Mason), Vol. 4B, Academic, 1966 (Russ. transl. Mir, 1970, p. 13).

[6] S. A. Al'tshuler, B. I. Kochelaev, and A. A. Leushin, Usp. Fiz. Nauk 75, 459 (1961) [Sov. Phys.-Usp. 4, 880 (1962)].

[7] L. D. Landau and E. M. Lifshitz, a) Teoriya uprugosti (Theory of Elasticity), Nauka, 1965; b) Elektrodinamika sploshnykh sred (Electrodynamics of Continuous Media), Gostekhizdat, 1957 [transl. publ. by Addison-Wesley].

[8] F. E. Borgnis, Phys. Rev. 98, 1000 (1955).

[9] F. I. Fedorov, Teoriya uprugikh voln v kristallakh (Theory of Elastic Waves in Crystals), Nauka, 1965.

[10] J. F. Nye, Physical Properties of Crystals, Oxford, 1964.

[11] K. Brugger, a) J. Appl. Phys. 36, 759 (1965); b) Phys. Rev. 137, 1826 (1965).

[12] P. C. Waterman, ibid. 113, 1240 (1959).

[13] J. de Klerk and M. J. P. Musrave, Proc. Phys. Soc. B68, 81 (1955).

[14] K. S. Aleksandrov, Kristallografiya 1, 718 (1956) [Sov. Phys.-Crystallogr. 1, 000 (1957)].

[15] E. P. Papadakis, J. Appl. Phys. 34, 2168 (1963); H. J. McSkimin and W. L. Bond, J. Ac. Soc. Am. 39, 499 (1966).

[16] D. L. Portigal and E. Burstein, Phys. Rev. 170, 673 (1968).

[17] A. S. Pine, ibid. B2, 2049 (1970).

[18] A. I. Akhiezer, Zh. Eksp. Teor. Fiz. 8, 1318 (1938).

[19] H. E. Bommel,and K. Dransfeld, Phys. Rev. 117, 1245 (1960).

[20] T. O. Woodruff and H. Ehrenreich, ibid. 123, 1553 (1961).

[21] W. Mason, a) see[5], vol. 3B, (Russ. transl.) 1968, p. 285; b) J. Ac. Soc. Am. 42, 253 (1967).

[22] H. H. Barrett and M. G. Holland, Phys. Rev. B1, 2538 (1970).

[23] R. C. Hanson, J. Phys. Chem. Sol. 28, 475 (1967).

[24] M. F. Lewis and E. Patterson, J. Appl. Phys. 39, a) 1913, b) 2469 (1968); c) Phys. Rev. 159, 703 (1967).

[25] L. G. Merkulov et al., Fiz. Tverd. Tela 11, 2769 (1969) [Sov. Phys.-Solid State 11, 2241 (1970)].

[26] M. J. Keck and R. J. Sladek, Phys. Rev. B2, 3135 (1970); Yu. Kh. Vekilov, et al., Fiz. Tverd. Tela 13, 1310 (1971) [Sov. Phys.-Solid State 13, 1095 (1971)].

[27] a) B. J. Miller, Phys. Rev. 132, 2477 (1963); b) B. Ya. Avdonin, V. V. Lemanov, et al., Fiz. Tverd. Tela 14, 877 (1972) [Sov. Phys.-Solid State 14, 747 (1972)].

[28] E. M. Ganapol'skiĭ and A. N. Chernets, Zh. Eksp. Teor. Fiz. 51, 383 (1966) [Sov. Phys.-JETP 24, 255 (1967)].

[29] D. W. Oliver and G. A. Slack, J. Appl. Phys. 37, 1542 (1966).

[30] L. D. Landau, Svornik trudov (Collected Works) Vol. 1, Nauka, 1969, p. 227.

[31] L. E. Gurevich and B. I. Shklovskiĭ, a) Fiz. Tverd. Tela 9, 526 (1967) [Sov. Phys.-Solid State 9, 401 (1967)]; b) Zh. Eksp. Teor. Fiz. 53, 1726 (1967) [Sov. Phys.-JETP 26, 989 (1968)].

[32]C. Herring, Phys. Rev. 95, 954 (1954).
[33]J. Ciccarello and K. Dransfeld, ibid.134,1517(1964).
[34]S. Simons, Proc. Phys. Soc. 82, 401 (1963).
[35]H. J. Maris, Phil. Mag. 9, 901 (1964).
[36]P. G. Kelemens, cf.[21a], (Russ. transl.) p. 244.
[37]S. L. McBride et al., J. Ac. Soc. Am. 45, 1385 (1969).
[38]M. Pomerantz, Phys. Rev. 139, 501 (1965).
[39]J. de Klerk and P. G. Klemens, ibid. 147, 585 (1966).
[40]R. Nava et al., ibid. 134, 581 (1964).
[41]J. de Klerk, ibid. 139, 1635 (1965).
[42]J. N. Lange, ibid. 176, 1030 (1968).
[43]P. C. Purdom and E. W. Prohofsky, ibid. 2B, 551 (1970).
[44]N. S. Shiren, Phys. Lett. 20, 10 (1966).
[45]V. L. Gurevich, a) Fiz. Tverd. Tela 4, 909 (1962) [Sov. Phys.-Solid State 4, 668 (1962)]; b) Fiz. Tekh. Poluprov. 2, 1557 (1968) [Sov. Phys.-Semicond. 2, 1299 (1969)]; B. I. Pustovoĭt, Usp. Fiz. Nauk 97, 257 (1969) [Sov. Phys.-Usp. 12, 105 (1969)].
[46]A. R. Hutson and D. L. White, J. Appl. Phys. 33, 40 (1962).
[47]R. Truell et al., ibid. 35, 1483 (1964); A. E. Lord, and R. Truell, ibid. 37, 4631 (1966).
[48]F. S. Hickernell, IEEE Trans. Sonics and Ultrasonics SU-13, 73 (1966).
[49]A. B. Sherman, I. I. Farbshteĭn, and V. V. Lemanov, Fiz. Tverd. Tela 12, 1765 (1970) [Sov. Phys.-Solid State 12, 1397 (1970)].
[50]A. B. Sherman and V. V. Lemanov, ibid. 13, 1690 (1971) [13, 1413 (1971)].
[51]P. J. Jorgensen and R. W. Bartlett, J. Phys. Chem. Sol. 30, 2639 (1969).
[52]D. L. White, J. Appl. Phys. 33, 2547 (1962).
[53]J. H. McFee, cf.[5], Vol. 4A, 1969, (Russ. transl.), p. 3.
[54]R. Truell, C. Elbaum, and B. Chick, Ultrasonic Methods in Solid State Physics, N. Y.—L., Academic Press, 1969
[55]T. Fitzberald et al., J. Appl. Phys. 35, 1639 (1964).
[56]K. R. Keller, ibid. 38, 3777 (1967).
[57]V. V. Lemanov et al., ZhETF 12, 515 (1970) [JETP Lett. 12, 360 (1970)].
[58]H. J. Maris, Phys. Rev. 175, 1077 (1968).
[59]J. N. Lange, ibid. 179, 860 (1969).
[60]L. G. Merkulov and L. A. Yakovlev, Akust, Zh. 6, 244 (1960) [Sov. Phys.-Acoust 6, 239 (1960)]; O. A. Mitchell, J. Appl. Phys. 36, 2083 (1965).
[61]A. I. Ahkiezer, V. G. Bar'yakhtar, and S. V. Peletminskiĭ, Spinovye volny (Spin Waves), Nauka, 1967; b) Zh. Eksp. Teor. Fiz. 35, 228 (1958) [Sov. Phys. JETP 8, 157 (1959)]; E. A. Turov and Yu. P. Irkhin, Fiz. FMM 3, 15 (1956); C. Kittel, Phys. Rev. 110, 836 (1958).
[62]R. C. LeCraw and R. Comstock, see[21a] (Russ. transl.), p. 156.
[63]E. Schlomann, J. Appl. Phys. 31, 1647 (1960).
[64]V. V. Lemanov et al., Zh. Eksp. Teor. Fiz. 59, 712 (1970) [Sov. Phys.-JETP 32, 389 (1971)].
[65]H. Matthews and R. Le Craw, Phys. Rev. Lett. 8, 397 (1962).
[66]B. Lüthi and F. Oertle, Phys. kondens. Materie 2, 99 (1964); G. A. Smolenskii and A. Nasyrov, Fiz. Tverd. Tela 7, 3704 (1965) [Sov. Phys.-Solid State 7, 3002 (1966)]; M. F. Lewis and D. G. Scotter, Phys. Rev. Lett. A28, 309 (1968).
[67]B. Lüthi, a) Phys. Lett. 3, 285 (1963); Appl. Phys. Lett. b) 6, 234 (1965); c) 8, 107 (1966).
[68]K. V. Goncharov et al., Fiz. Tverd. Tela 9, 3384 (1967) [Sov. Phys.-Solid State 9, 2671 (1968)].
[69]V. V. Lemanov et al., ZhETF Pis. Red. 8, 242 (1968) [JETP Lett. 8, 148 (1968)].
[70]R. Guermeur et al., Sol. State Comm. 5, 369 (1967).
[71]V. V. Lemanov and A. V. Pavlenko, Zh. Eksp. Teor. Fiz. 57, 1528 (1969) [Sov. Phys.-JETP 30, 826 (1970)].
[72]A. V. Pavlenko, Yu. M. Yakovlev, and V. V. Lemanov, Fiz. Tverd. Tela 11, 3300 (1969) [Sov. Phys.-Solid State 11, 2673 (1970)].
[73]B. A. Auld et al., Appl. Phys. Lett. 9, 436 (1966); H. van de Vaart and H. D. Smith, ibid., p. 439.
[74]J. R. Franz and B. Lüthi, Sol. State Comm. 5, 319 (1967).
[75]I. L. Fabelinskiĭ, Molekulyarnoe rasseyanie sveta (Molecular Scattering of Light), Nauka, 1965.
[76]S. M. Rytov, Zh. Eksp. Teor. Fiz. 5, 843 (1935).
[77]R. W. Dixon, IEEE J. Quantum Electron. QE-3, 85 (1967); V. V. Lemanov and O. V. Shakin, ZhETF Pis. Red. 13, 549 (1971) [JETP Lett. 13, 392 (1971)]; Fiz. Tverd. Tela 14, 229 (1972) [Sov. Phys.-Solid State 14, 184 (1972)].
[78]D. F. Nelson and M. Lax, a) Phys. Rev. Lett. 24, 379 (1970); b) Phys. Rev. 3B, 2778 (1971).
[79]D. F. Nelson and P. D. Lazay, Phys. Rev. Lett. 25, 1187 (1970).
[80]O. V. Kachalov, ZhETF Pis. Red. 13, 109 (1971) [JETP Lett 13, 75 (1971)].
[81]R. W. Damon et al., Physical Acoustics, v. 7, ed. by W. P. Mason and R. N. Thurston, N. Y.—L. Academic Press, 1970, p. 273.
[82]V. V. Lemanov, O. V. Shakin, and G. A. Smolenskiĭ, Fiz. Tverd. Tela 13, 533 (1971) [Sov. Phys.-Solid State 13, 426 (1971)].
[83]R. W. Dixon, J. Appl. Phys. 38, 5149 (1968).
[84]E. I. Venturini et al., ibid. 40, 1622 (1969).
[85]D. A. Pinnow and R. W. Dixon, Appl. Phys. Lett. 13, 156 (1968).
[86]N. Uchida and Y. Ohmachi, J. Appl. Phys. 40, 4692 (1969).
[87]O. G. Farah et al., ibid., p. 2365.
[88]B. A. Richardson, et al., J. Ac. Soc. Am. 44, 1608 (1968); 1189 (1972); O. V. Shakin and V. V. Lemanov, Fiz. Tverd. Tela 14, 1384 (1972) [Sov. Phys.-Solid State 14, 1189 (1972)].
[89]D. E. Caddes et al., Appl. Phys. Lett. 8, 309 (1960).
[90]R. Y. Chiao et al., Phys. Rev. Lett. 12, 592 (1964).
[91]L. K. Zarembo and V. A. Krasil'nikov, Usp. Fiz. Nauk 102, 549 (1970) [Sov. Phys.-Usp. 13, 778 (1971)].
[92]H. H. Barrett, cm[81], v. 6, 1968, p. 65

Translated by J. G. Adashko